

# POLITECNICO DI TORINO

Collegio di Ingegneria Chimica e dei Materiali

**Corso di Laurea Magistrale  
in Ingegneria dei Materiali**

Master's degree thesis

## **Vanillin bio-based reprocessable polymers**



**Politecnico  
di Torino**

### **Supervisors:**

Professor Marco Sangermano

Professor Minna Hakkarainen

Dott. Sathiyaraj Subramaiyan

### **Candidate**

Matteo Bergoglio

July 2022



# Table of Contents

<b>Abstract</b>	I
<b>Chapter 1: Introduction</b>	1
<i>1.1 Polymers</i>	2
<i>1.2 Thermoplastics and thermosets</i>	4
<i>1.3 Covalent Adaptable Network (CANs)</i>	5
<i>1.4 Vitrimer-like polymers</i>	7
<b>Chapter 2: Experimental</b>	11
<i>2.1 Materials</i>	11
<i>2.2 Monomer synthesis</i>	11
<i>2.2.1 Monomer precursor synthesis (3)</i>	11
<i>2.2.2 Monomer synthesis (5)</i>	12
<i>2.2.3 Monomer synthesis (7)</i>	13
<i>2.3 Polymer synthesis</i>	14
<i>2.3.1 Thermoplastics</i>	14
<i>2.3.2 Vitrimers</i>	15
<i>2.4 Characterization methods</i>	18
<i>2.4.1 Qualitative analysis – ATR-FTIR, NMR, SEC analysis</i>	18
<i>2.4.2 Thermal and mechanical properties -TGA, DSC, DMA analysis and tensile testing</i>	22
<b>Chapter 3: Results and discussion</b>	27
<i>3.1 Monomer synthesis</i>	27
<i>3.2 Thermoplastic polymers synthesis</i>	34
<i>3.2.1 Synthesis of Polyurethane (P5a)</i>	34
<i>3.2.2 Synthesis of Polyester (P5b)</i>	39
<i>3.3 Thermoset polymers synthesis - vitrimers</i>	43
<i>3.3.1 Synthesis of Vitrimer 1 (9)</i>	43
<i>3.3.2 Synthesis of Vitrimer 2 (11)</i>	51

3.3.3 <i>Synthesis of Vitrimer 1 (9) and Vitrimer 2 (11) with different ratio</i>	60
3.4 <i>Thermoset polymers – reprocessing</i>	65
<b>Chapter 4: Conclusions</b>	69
<b>Bibliography</b>	73





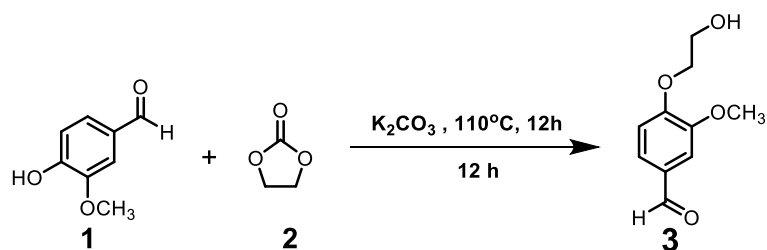


## Abstract

La presente tesi riguarda la sintesi e la caratterizzazione di quattro polimeri bio-based, contenenti legami imminici utili alla degradazione. I polimeri sintetizzati comprendono due termoplastici, un poliestere ed un poliuretano, e due termoindurenti.

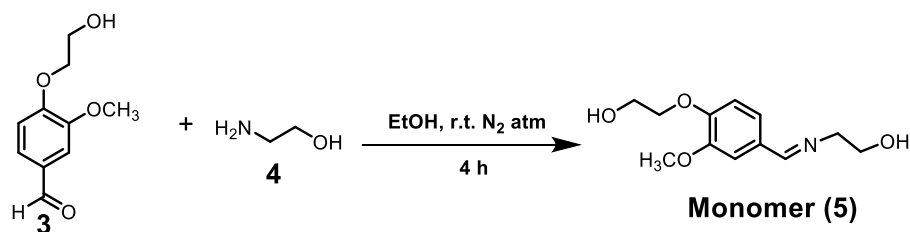
Tutti i materiali sono prodotti a partire dalla vanillina, composto naturale essere estratto direttamente dalle piante oppure sintetizzato chimicamente a partire da eugenolo, o lignina.

Come visibile in Schema 1, la vanillina è stata fatta reagire con etilene carbonato per ottenere vanillina estesa, molecola di partenza dalla quale sono stati sintetizzati tutti i prodotti finali. Questa prima sintesi è stata eseguita per ottenere una molecola più reattiva della vanillina stessa, grazie all'introduzione di una catena alifatica nella struttura. L'ottenimento del composto è stato confermato da analisi  $^1\text{H}$  NMR e  $^{13}\text{C}$  NMR, visibili in Figure 17 e 18, e dall'analisi FTIR, visibile in Figure 19.

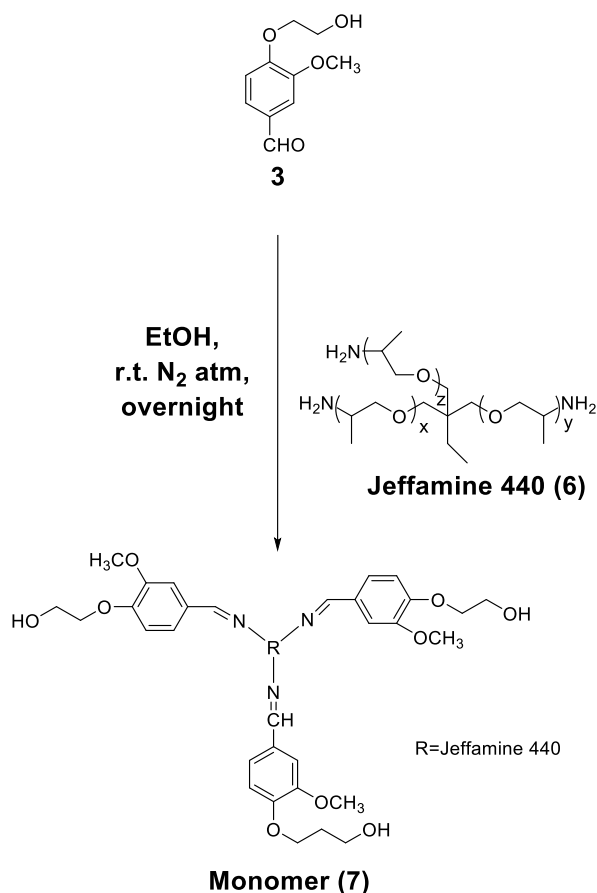


Schema 1. Sintesi del composto (3).

Facendo reagire la vanillina estesa con due diversi reagenti sono stati sintetizzati due monomeri che possiedono gruppi amminici nella struttura. Il primo monomero è stato ottenuto tramite reazione con amminoetanolo (Schema 2), mentre il secondo monomero è stato ottenuto grazie alla reazione con Jeffamine 440, una tri-ammina (Schema 3).



Schema 2. Sintesi del monomero (5).



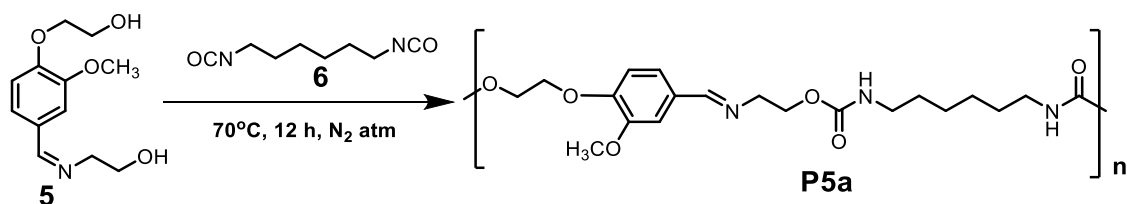
**Schema 3. Sintesi del monomero (7).**

I monomeri sintetizzati sono stati caratterizzati tramite differenti prove. Sono state eseguite analisi qualitative <sup>1</sup>H NMR, <sup>13</sup>C NMR e FTIR del primo (5) e del secondo monomero (7) (Figure 20,21,22, 24,25), che hanno confermato l'ottenimento delle strutture desiderate.

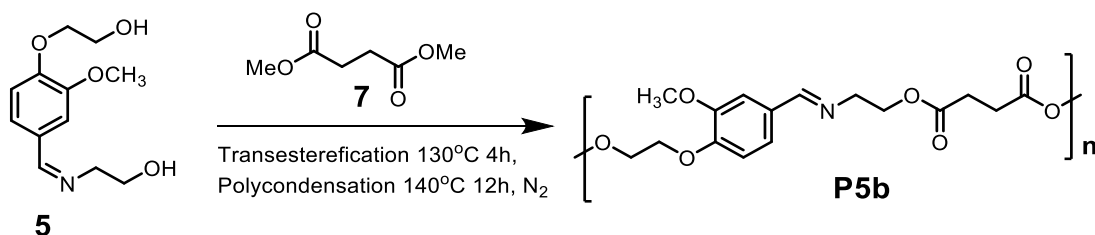
In seguito, è stata eseguita l'analisi TGA (Figure 23 e 26) che ha mostrato una buona resistenza termica di entrambi i materiali, con un inizio di degradazione per il monomero (5) intorno ai 230 °C, mentre per il monomero (7) intorno ai 310 °C. La maggiore resistenza termica riscontrata nel secondo monomero è dovuta alla maggiore presenza di gruppi aromatici nella struttura, che si traduce in una minore percentuale di residuo carbonioso al termine della prova (17% circa), se confrontata con il monomero (5), il quale presenta un residuo intorno al 30%.

I monomeri sono stati a loro volta il punto di partenza di sintesi dei polimeri.

Come visibile in Schema 4, a partire da monomero (5) ed esametilene diisocianato, è stato sintetizzato il poliuretano (P5a), mentre sostituendo al diisocianato il dimetilsuccinato è stato sintetizzato il poliestere (P5b) (Schema 5).



Schema 4. Sintesi del poliuretano (P5a).



Schema 5. Sintesi del poliestere (P5b).

I polimeri termoplastici sono stati caratterizzati qualitativamente tramite analisi  $^1\text{H}$  NMR, FTIR e DSC (Figure 27,28,33,34,35,37). È possibile osservare dall'analisi FTIR del poliuretano (P5a) la scomparsa del gruppo -OH del monomero (5) e diminuzione del gruppo C=N, segno di avvenuta reazione, e la comparsa dei gruppi caratteristici come i picchi corrispondenti al legame uretanico -NH e carbonile C=O. Allo stesso modo, dall'analisi FTIR del poliestere (P5b) si nota la scomparsa del gruppo ossidrilico del monomero (5), la diminuzione del gruppo C=N, e la comparsa del gruppo carbonile C=O tipico del poliestere. L'analisi TGA ha mostrato una buona resistenza termica di entrambi i polimeri, con una temperatura di iniziale degradazione intorno ai 250 °C (Figure 31 e 35). Il poliuretano (P5a) possiede tre diversi step di degradazione. Il primo step potrebbe corrispondere alla rottura del legame imminico, il secondo al legame uretanico, il terzo al legame etere o estere. Il poliestere (P5b) possiede invece due step di degradazione; il primo potrebbe corrispondere alla rottura del legame imminico ed il secondo alla rottura del legame etere o estere.

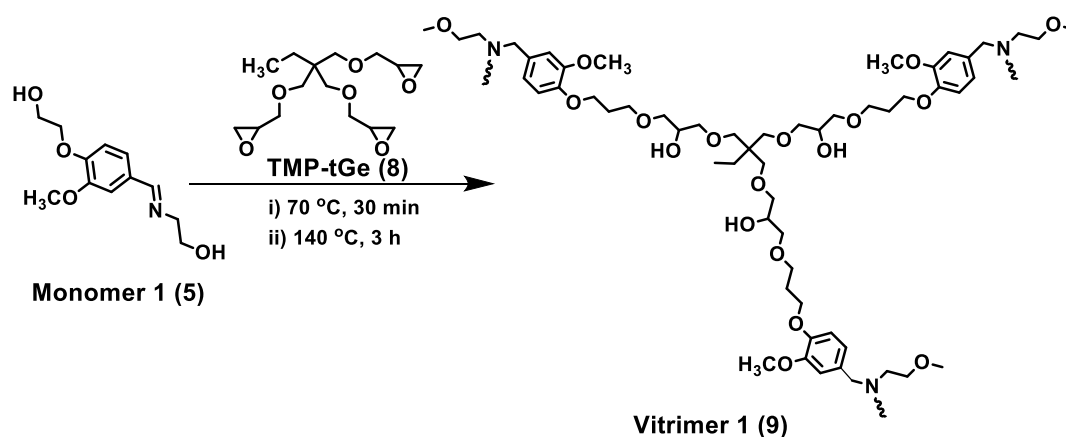
Con l'intenzione di trovare il peso molecolare medio dei materiali è stata eseguita l'analisi SEC (Figure 29 e 36), la quale ha mostrato una massa molecolare media numerale  $M_n$  sopra i 10 000 g mol $^{-1}$  per entrambi i polimeri, valore comparabile ai polimeri convenzionali riportati in letteratura.

La temperatura di transizione vetrosa è stata ricavata dall'analisi DSC (Figure 30 e 37), e risulta maggiore nel poliuretano (55 °C) rispetto al poliestere (29 °C). Questo valore è

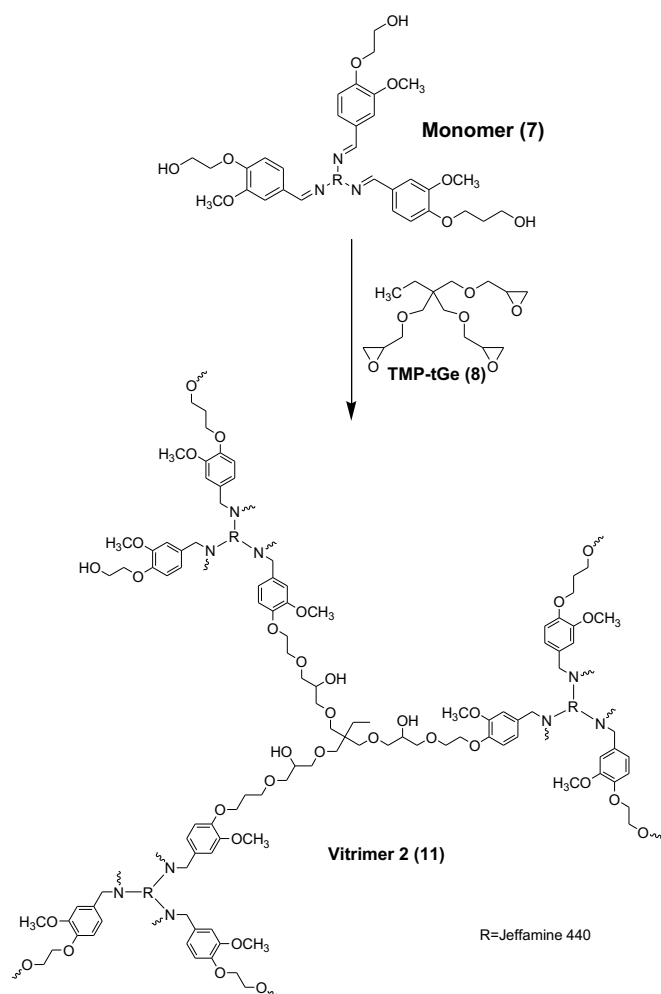
dato dalla maggiore rigidità del poliuretano conferita dal gruppo -NHCOO e dal maggiore valore della massa molecolare media numerale  $M_n$ .

È stata eseguita la prova di riciclo chimico per il poliuretano (P5a), immergendo il materiale all'interno di una soluzione acida 0.1M di HCl per 24 h (Figura 32). Il processo è stato monitorato durante il tempo tramite analisi  $^1\text{H}$  NMR. Al termine delle 24 ore è possibile osservare nello spettro la comparsa dei picchi caratteristici dei precursori come il gruppo aldeidico -CHO ed i gruppi aromatici ed alifatici.

Le sintesi dei materiali termindurenti, chiamati Vetrimeri grazie alla struttura contenente gruppi imminici, sono visibili in Schema 6 e Schema 7. La sintesi ha coinvolto il monomero (5) e trimetilolpropano-triglicidil etere (TMP-TGE) per il Vetrimer (9), ed il monomero (11) e TMP-TGE per il Vetrimer (12), con una reticolazione attivata tramite calore.



Schema 6. Sintesi del Vetrimer (9).



**Schema 7. Sintesi del Vitrimero 2 (12).**

La conferma di avvenuta reticolazione è stata fornita da analisi FTIR (Figure 38 e 50), dove si nota in entrambi i casi un incremento dei gruppi ossidrili secondari ed una diminuzione di intensità del picco appartenente al legame C=N. Nel grafico FTIR riguardante il Vitrimero (9) è anche possibile osservare la scomparsa del gruppo ossidrile primario.

Le analisi termogravimetriche rappresentate in Figure 40 e 52 mostrano una buona resistenza termica dei due materiali con picchi di massima velocità di degradazione intorno ai 300°C. Il grafico riguardante il Vitrimero (12) possiede un solo picco di degradazione come previsto, mentre il Vitrimero (9) presenta due picchi distinti di

degradazione, dove il picco a temperatura inferiore può essere attribuito alla degradazione di monomero non reagito.

È stato eseguito il gel content test immergendo i campioni per tre giorni all'interno di soluzioni di etanolo EtOH e Tetraidrofurano THF, i quali solubilizzano entrambi i monomeri di partenza. La prova ha restituito valori di gel content intorno al 94% per il Vetrimer (9) ed intorno al 77% per il Vetrimer (12). Il minore valore di gel content nel secondo termoindurente può essere dovuto al maggiore ingombro sterico che possiede il monomero (11), il quale impedisce la reazione di tutti i suoi gruppi funzionali creando oligomeri che vengono quindi solubilizzati nei solventi.

Il test di resistenza chimica a solventi è visibile in Figure 46 e 58. Entrambi i polimeri hanno mostrato, da un'analisi visiva, una buona resistenza a tutti i solventi utilizzati, eccezion fatta per DMSO e DMF, che hanno parzialmente disciolto i campioni dopo due giorni.

Il test di riciclo chimico è stato eseguito immergendo i campioni in soluzione di HCl 0.1M per due ore, provocando una completa dissoluzione di entrambi (Figure 47). Seguendo la degradazione tramite  $^1\text{H}$  NMR nel tempo, è confermato l'ottenimento dei picchi caratteristici dei precursori (Figure 48 e 59).

Per avere un'indicazione della percentuale di conversione dei gruppi funzionali dei monomeri sono state eseguite analisi DSC della miscela di reazione. È stata eseguita inizialmente un'analisi DSC dinamica (curve rosse in Figure 43 e 55), dalla quale si è calcolato l'integrale appartenente al picco della curva, corrispondente all'entalpia totale di conversione dei gruppi epossidici. Una seconda analisi DSC, questa volta in isoterma, è stata eseguita alla temperatura corrispondente alla massima temperatura del picco ottenuto dalla DSC dinamica. Dalla seconda analisi, è stata calcolata, sempre considerando l'integrale della curva, l'entalpia effettiva di reazione dalla quale si può dedurre la conversione della miscela di reazione dividendo l'entalpia effettiva per l'entalpia teorica. La miscela appartenente al Vetrimer (9) ha fornito 42% di conversione, per il Vetrimer (12) si ha 50% di conversione.

Le analisi di caratterizzazione meccanica hanno compreso prove di trazione e DMA.

Le prove di trazione, rappresentate in Figure 42,53, Table 3,5, forniscono un maggiore modulo elastico nel Vetrimer (12). Questo è probabilmente dovuto alla maggiore percentuale di conversione che quest'ultimo possiede, dimostrata dall'analisi DSC eseguita sulla miscela di reazione.



Le analisi DMA, visibili in Figure 41 e 53, hanno ugualmente mostrato maggiore modulo conservativo nel Vetrimer (12) prima della  $T_g$ . Anche questo comportamento può essere spiegato dalla maggiore percentuale di conversione della miscela. A temperature maggiori della  $T_g$  si ha un comportamento opposto; infatti, il modulo conservativo è minore nel Vetrimer (12), dovuto ad una minore densità di reticolazione di quest'ultimo se confrontato con il Vetrimer (9).

Allo scopo di migliorare il prodotto finale, sono state eseguite diverse sintesi variando la ratio dei composti di partenza, come visibile in Table 8,10, e Figure 61,66. Tutte le formulazioni sono state analizzate tramite analisi DSC (Figure 62 e 67), dalla quale è constatabile che la temperatura di transizione vetrosa non varia considerevolmente al variare della ratio dei reagenti. È comunque possibile rilevare una diminuzione della  $T_g$  nei campioni contenenti un eccesso di monomero nel Vetrimer (9), comportamento attribuibile alla minore percentuale di reticolazione ottenuta in mancanza di reagente reticolante. Il Vetrimer (12) possiede un comportamento opposto, probabilmente dovuto all'incremento della porzione alifatica della struttura ottenuta con eccesso di TMP-TGE. Quasi tutti campioni sintetizzati con differenti ratio hanno presentato scarse caratteristiche meccaniche, rendendo impossibili caratterizzazioni meccaniche più accurate come prove di trazione o analisi dinamo meccaniche DMA. L'unico campione con caratteristiche adeguate ad essere testato meccanicamente è stato il Vetrimer (9) con eccesso di 1.1 TMP-TGE, che comunque è risultato possedere inferiori caratteristiche meccaniche rispetto all'originale, anche se il valore del modulo conservativo maggiore rispetto al Vetrimer (9) originale (4.0 MPa contro 2.6 MPa) denota una maggiore reticolazione data dall'eccesso di TMP-TGE (Figure 64 e 65, Table 9).

Entrambi i Vetrimeri sono stati riprocessati meccanicamente. Il riprocessamento è stato eseguito riducendo in porzioni di circa 5 mm i campioni e ponendoli in una pressa a caldo a 130°C sotto pressione (Figure 69 e 70). Le formulazioni di Vetrimer (9) e Vetrimer (9) con eccesso di TMP-TGE sono state caratterizzate nuovamente meccanicamente dopo l'operazione, mentre il Vetrimer (12) riprocessato è risultato non adeguato alla caratterizzazione. I campioni riprocessati hanno entrambi mostrato maggiore rigidità, quindi maggiore modulo elastico, e minore duttilità (Figure 71 e 72, Table 11,12), proprietà dovute ad un incremento della densità di reticolazione avvenuta all'interno della pressa a caldo.

Concludendo, sono stati sintetizzati due polimeri termoplastici Schiff-base e due Vetrimeri con successo, come dimostrato dalle analisi NMR e FTIR. Tutti e quattro i materiali hanno presentato buona resistenza termica, ed il legame imminico ha permesso un facile riciclo chimico in condizioni debolmente acide per tutti i polimeri; in aggiunta, i Vetrimeri possono essere riprocessati meccanicamente tramite pressa a caldo. Le caratteristiche ottenute avvalorano i polimeri sintetizzati come una valida alternativa ai polimeri tradizionali derivati da fonti fossili; in aggiunta, i materiali termoindurenti possono raggiungere un completo recupero al termine del loro utilizzo, compito impossibile nei termoindurenti convenzionali.





## **Chapter 1: Introduction**

This thesis has the synthesis and characterization of biobased polymers with imine groups that allow recycling as the primary goal.

The project is developed entirely in Kungliga Tekniska högskolan (KTH Royal Institute of Technology), in the department of Fibre and Polymer Technology (FPT).

The work is focused on synthesizing four different polymers, two thermoplastic polymers, polyester and polyurethane, and two thermoset polymers, followed by their characterization. All the polymers are manufactured starting from vanillin, a natural compound.

The first section of the thesis describes the synthesis methods. Consequently, the chapter “Results and Discussion” describes the quality characterizations and the mechanical characterizations of the obtained products.

Lastly are exposed the conclusions regarding the work done.

## 1.1 Polymers

Polymers, commonly called “plastics”, have become an essential material for the modern economy due to their low cost and unique physical and mechanical properties. Easy processing, versatility, durability, high elasticity values, tensile strength to weight ratio, and heat stability are just some of their properties. Their use increased twenty times during the last 50 years, from 1.5 million tonnes in 1950 to 367 tonnes in 2020 (Figure 1). Furthermore, the prediction says that their use will double in the next 20 years [1,2].

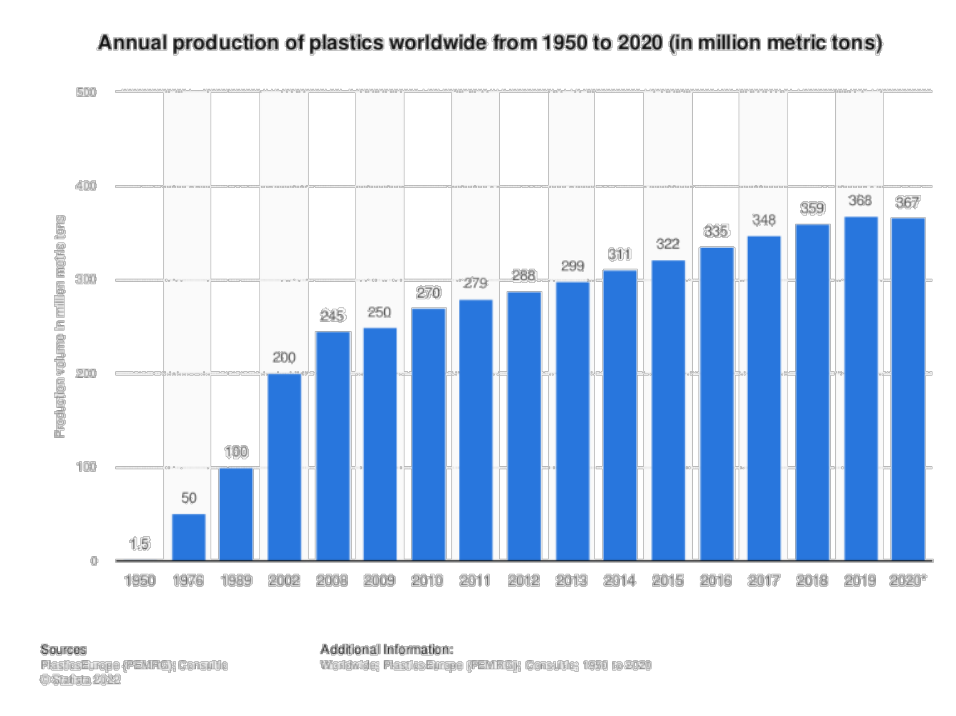


**Figure 1. Annual production of plastic worldwide during years [3].**

Despite their properties, the utilization of polymers brings various issues that are becoming noticeable day after day. For example, after brief use, 95% of packaging polymers become ready to be sent to landfills due to their single-use purpose. Only 14% of them are collected to be recycled, and if it is considered the reprocessing losses, only 5% are effectively recycled. Furthermore, recycled plastics usually have lower properties and values than virgin material, they are no more recycled, and ultimately, they find their way to landfills or pollute the environment [4].

These drawbacks induce the scientific community to find new recycling ways and new green-based polymers, to reduce the impact of polymers on the environment, leading to new challenges. The main target is to obtain polymers that can be easily recycled and not persist in the environment. However, simultaneously they have to be sufficiently resistant to be used in their application.

In the past decade, a sustainable recycling way it has been proposed. This alternative strategy suggests collecting and recycling chemically polymers sent to disposal into monomers, allowing to create new polymers without using new monomers, leading to a circular material economy [5].

Polymers can be classified using different criteria, but in this project, it has been studied reprocessability, recyclability, and mechanical properties according to temperature. Based on thermal properties, polymers can be classified into two classes: thermoplastics and thermosets.

## ***1.2 Thermoplastics and thermosets***

Thermoplastic materials can flow under the action of heat and pressure. This property makes them easily manufacturable, representing 80% of the total polymeric materials used nowadays [6].

They are made by long chains of high molecular mass that are not held together by chemical bonds but from physical entanglements. The chains increase their mobility upon heating and can flow with a viscosity drop. Upon cooling, the chains become again stable, assuming the shape of the mold. This process can happen several times without any critical damage, making the thermoplastic recyclable and reprocessable.

The degree of crystallinity of those polymers can influence their properties. Both semi-crystalline and amorphous thermoplastics at  $T > T_g$  behave like a viscous liquid, while at  $T < T_g$ , they act as hard and rigid glasses [7].

Unlike thermoplastics, thermosets materials cannot flow under the action of heat and pressure due to their three-dimensional structure made by crosslinked solid bonds. The bonds are formed during the curing process, made by heating or by adding a curing agent. They give the thermosets a stable, rigid, and robust structure appropriate for applications like construction and building, transportation, adhesives, and electrical equipment. If combined with carbon fibers and glass to make composites, it is also possible to use them in advanced applications, mainly in aerospace and military industries.

Their excellent properties give them a downside, thermosets cannot be reshaped and recast because, during heating, the degradation of the material occurs before reaching an optimal flow suitable for reshaping, preventing the recycling. [6,8].

An interesting strategy for dealing with these issues is given by introducing exchangeable chemical bonds, which form a dynamic crosslinked structure. If chemical crosslinks can be exchanged efficiently and reliably between different positions along the polymer chain, macroscopic flow can be obtained without losing neither material nor structural properties.

Polymers that shows these properties are known as CANs or covalent adaptable network [9]; their properties can potentially fill the gap between thermoset and thermoplastic.



### 1.3 Covalent Adaptable Network (CANs)

CANs can also be classified into two different groups that are characterized by their exchange mechanism.

The first group has dissociative dynamic bonds. The mechanism consists of breaking the crosslinked bonds to form them again in another network position (Figure 2).

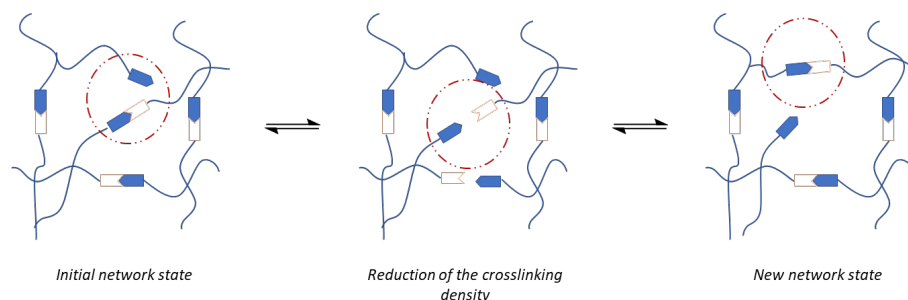


**Figure 2. Dissociative dynamic bonds [10].**

When crosslinks are broken, the gel content is reduced, leading to a loss of network connectivity or even complete depolymerization. Depending on the chemical structure, the result of the breaks can lead to the complete recovery of monomers or obtain free chains. The best-known example of dissociative CANs regards reversible Diels-Alder reaction between furans and maleimides (Figure 3).

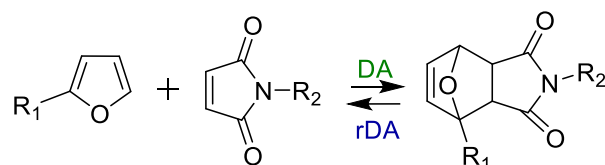


**Figure 3. Reversible Diels-Alder reaction implying furan and maleimide [10].**

Upon heating, the reaction becomes reversible, increasing the number of breaking/forming bonds, leading to a decrease in connectivity, allowing a fast topology rearrangement. This loss in the crosslinked bonds results in a viscosity drop, giving a thermoplastic-like behavior. Upon cooling, the bonds are formed again in the same amount of the starting material, giving the initial thermosetting properties.

The second group has associative dynamic bonds. In this case, the crosslinked density is fixed when equilibrium is reached. While the crosslinked bonds are breaking, the new bonds are forming simultaneously [11].

This process can happen in two ways: stepwise or concerted (Figure 4).

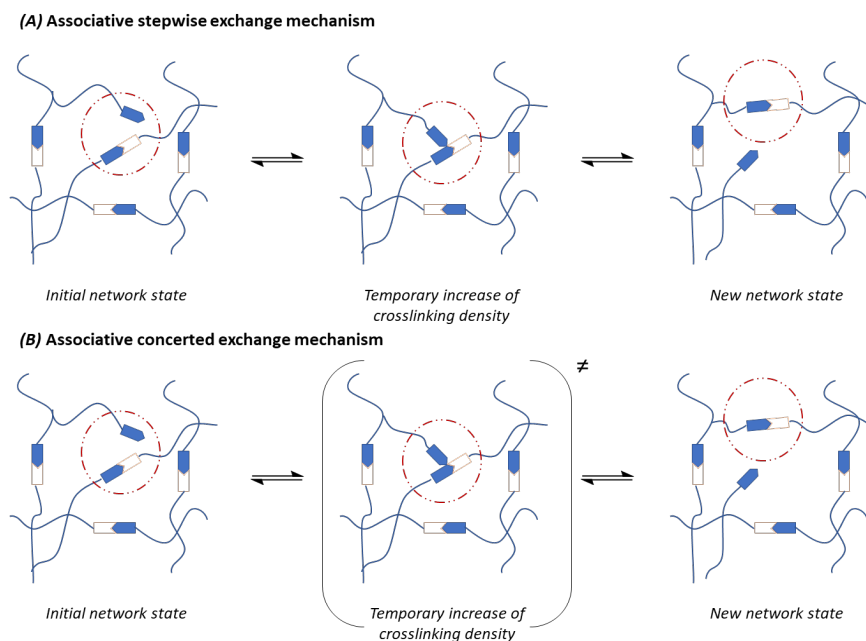


**Figure 4. Stepwise (A) and concerned (B) mechanism of associative dynamic bonds [10].**

Figure 4 represents the exchange mechanism in the absence of a catalyst, but this is often required to obtain the reaction. In the associative stepwise exchange mechanism, the reaction occurs by forming a short-lived intermediate, giving at the beginning an addition reaction and after an elimination reaction. In the second scenario, the process happens in a single step (transition state) without involving any intermediate.

Such systems have an issue regarding reversibility: unavoidable termination reactions happen during the formation and breaking of the bonds.

One possible solution to this issue comes from a particular class of associative CANs: Leibler and co-workers in 2011 introduced thermosets polymers with associative dynamic bonds based on a transesterification reaction named Vitrimers, thanks to the similarity of some of their properties with vitreous silica.

Vitrimers differ from dissociative CANs due to the permanent network. The network can be rearranged thanks to the transesterification reaction (exchange reaction) once heated, leading from a viscoelastic solid to a viscous liquid while maintaining a constant amount of crosslinked bonds. This allows the material to be reprocessed, reshaped, and healed without changing its properties [12].

### 1.4 Vitrimer-like polymers

It has been observed that also dissociative CANs can behave like Vitrimers, showing an Arrhenius viscosity relationship during stress relaxation experiments without any viscosity drop during the exchange of covalent bonds. They also show a rubbery plateau at high temperature after  $T_g$ . Those features make them hard to be distinguished from the proper Vitrimers; hence they are called Vitrimer-like polymers [13,14].

Vitrimer-like polymers, upon heating, have a higher rate of reassociation bonds than dissociation. Under this condition, they have the rheological behavior of Vitrimers, and they can also be recycled using grinding and hot-press.

The central difference with respect to Vitrimers is observed in the possibility of dissolving them partially or entirely in specific solvents at a certain temperature. Chemical recycling is therefore an alternative route to hot-press recycling, that could make Vitrimer-like polymers more sustainable than Vitrimer [15].

The most crucial feature of Vitrimers regards their malleability to high temperature, caused by the redistribution of the dynamic linkages through the network, hence a lower viscosity. When the temperature is high enough to permit fast exchange reactions, the exchange reactions control the viscosity. The drop-in viscosity opens new ways to recycle thermosets: they can also be recycled at high temperatures only using hot-press. Hot-press reprocessing is done by cutting them into small pieces before using the machine. At the end of the process, polymers with comparable properties to the original ones are obtained [11].

According to an Arrhenius law, the viscosity of the polymers decreases with the rising of the temperature (Figure 5).

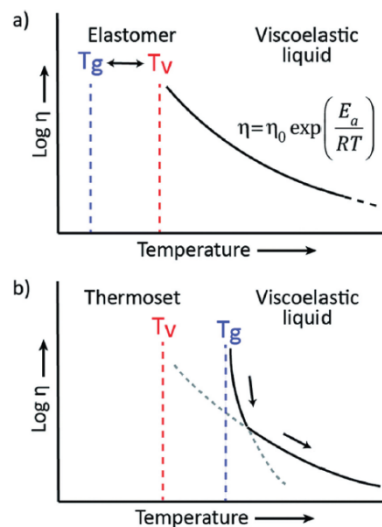


Figure 5. Viscoelastic behavior of vitrimers [11].

In order to describe the behavior based on the viscoelastic nature of Vitrimers, it has been created a new transition temperature called  $T_v$ , topology freezing temperature. Above  $T_v$ , the viscous flow occurs, while below  $T_v$ , the network topology appears frozen because the kinetics of the exchange reaction is too slow, and the material behaves like a thermoset.  $T_v$  is defined as the temperature at which the viscosity of the polymer is  $10^{12}$  Pa s. (Figure 5). It is possible to distinguish two different scenarios based on the value of  $T_v$ , which can be above or below  $T_g$ . In both cases, the exchange reaction occurs above  $T_g$  because the polymer is in a glassy state under this temperature.

In the first case, if  $T_v > T_g$ , the polymer behaves like a classic thermoset before reaching  $T_v$ , changing its state from glassy to rubbery after reaching  $T_g$ . When  $T_v$  is reached, the exchange reactions are fast enough to modify the topology of the polymer, and the material behaves like a viscoelastic liquid following the Arrhenius law.

If  $T_v < T_g$ , the exchange reactions are present after reaching  $T_v$ , but the topology does not change until reaching  $T_g$  because the structure is trapped in the glassy matrix. Exceeding  $T_g$ , the viscosity first drops following the Williams–Landel–Ferry (WLF) model thanks to the high mobility of the chains; then, when the exchange reactions become predominant, it follows the Arrhenius law.

Even though Vitrimer can behave like thermosets before exceeding  $T_v$ , by increasing the temperature, they can be reshaped. This characteristic opens new ways for recycling, as mentioned in the previous paragraph. This also allows them to obtain self-healing properties [11].





## Chapter 2: Experimental

### 2.1 Materials

Vanillin (99%), ethylene carbonates (98%), potassium carbonates ( $K_2CO_3$ , 99%), sodium sulphate ( $Na_2SO_4$ ), dibutyltin oxide (DBTO) (>98%), 2-Aminoethanol (>99%), Trimethylolpropane tris [poly(propylene glycol), amine terminated] ether, Trimethylolpropane triglycidyl ether (TMP-TGE), 1,2-Dimethylimidazole, Dibutyltin dilaurate (DBTDL) (>95%), Hexamethylene diisocyanate (>99%), were purchased from Sigma-Aldrich.

*N*-dimethylformamide (DMF, ACS, Reag. Ph. Eur.), ethyl acetate (EtOAc, ACS, Reag. Ph. Eur.), ethanol (EtOH) were purchased from VWR Chemicals.

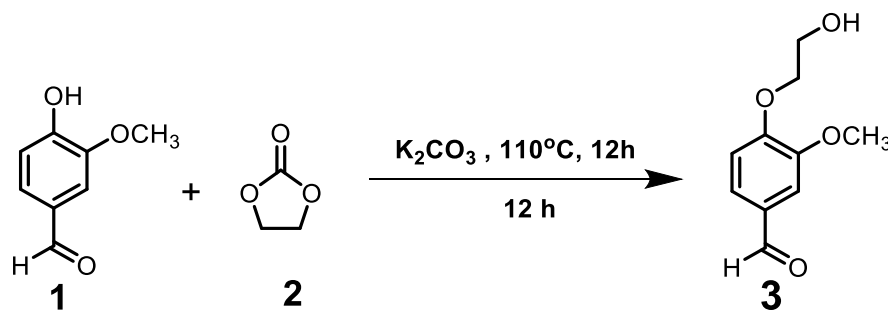
All chemicals and reagents were used as received.

### 2.2 Monomer synthesis

#### 2.2.1 Monomer precursor synthesis (3)

The first step involved a nucleophilic substitution reaction.

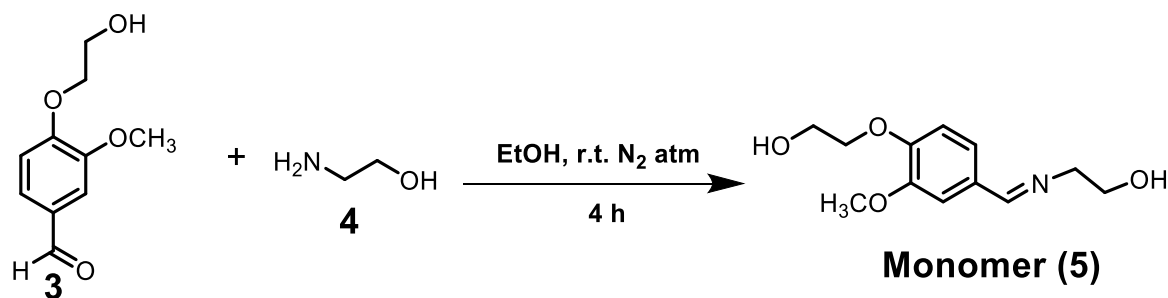
A solution of vanillin and ethylene carbonate in the presence of a base ( $K_2CO_3$ ) and DMF as a solvent, was kept at 110°C for 12 h under  $N_2$  atmosphere (scheme 1). The completion of the reaction was monitored using TLC. The reaction mixture was then extracted by using EtOAc with water (1:5), and then the organic layer was washed twice with water. Subsequently, the solution was dried with  $Na_2SO_4$  and concentrated by using rotavapor. The product was recrystallized by using hot water (60°C) in a conical with a stirrer; it was added gradually, then covered by aluminium; subsequently stored in the fridge for two days. The collected compound (yellow flakes) was completely dried in a vacuum oven at 60°C for 12 h. The yield of  $\geq 35\%$  is shown in scheme 1.



Scheme 1. Synthesis of compound (3).

### 2.2.2 Monomer synthesis (5)

In the second step, compound 3 was dissolved in EtOH, and a calculated amount of 2-amino ethanol was added dropwise. The solution was stirred at room temperature in the presence of N<sub>2</sub> atmosphere for 4 h, then the precipitate was filtered and washed with ethanol and dried by using vacuum pump for 12 h. A yellow powder was obtained. The yield of  $\geq 80\%$  is shown in scheme 2.

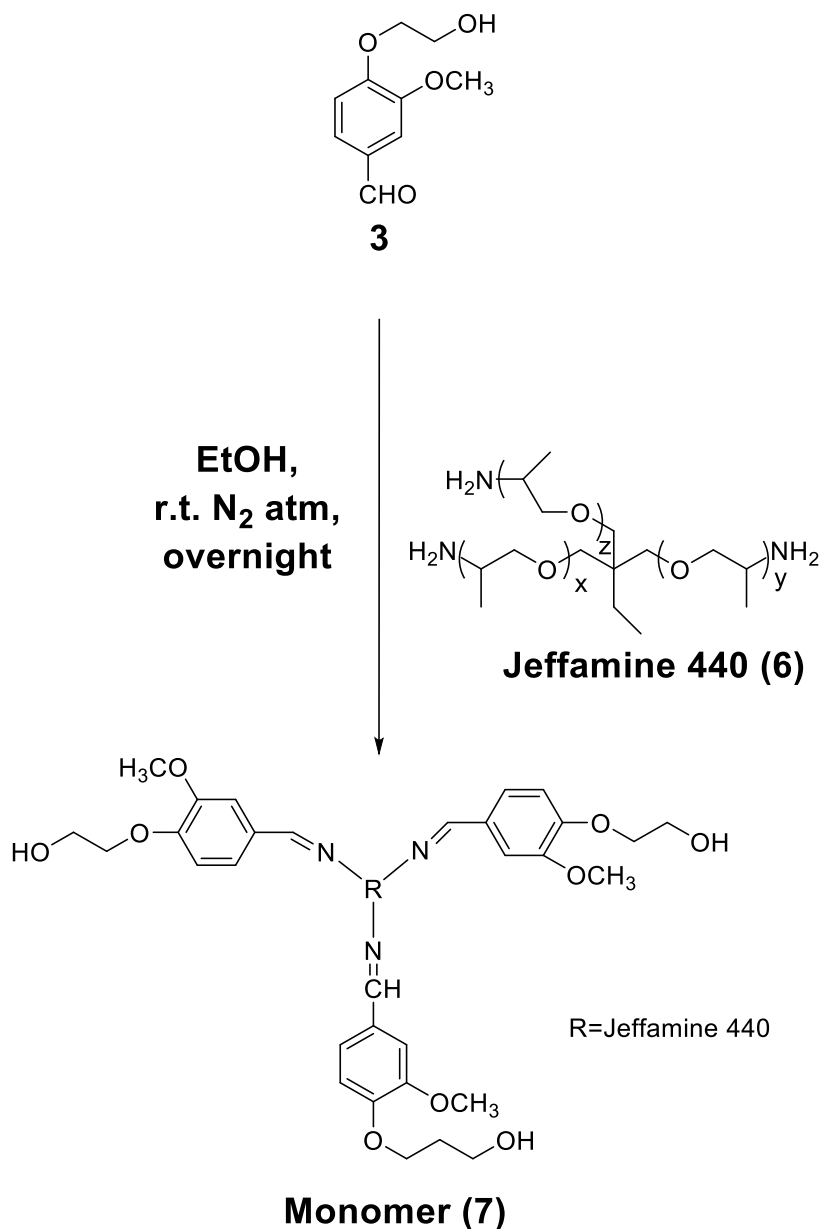


Scheme 2. Synthesis of monomer (5).



### 2.2.3 Monomer synthesis (7)

The compound 3 was dissolved in EtOH, and a calculated amount of trimethylolpropane tris [poly(propylene glycol), amine terminated] ether (Jeffamine 440) was added. The solution was stirred at room temperature in the presence of N<sub>2</sub> atmosphere overnight; then the precipitate was dried by using vacuum pump for 12 h. An orange viscous liquid was obtained. The yield of  $\geq 70\%$  is shown in scheme 3.



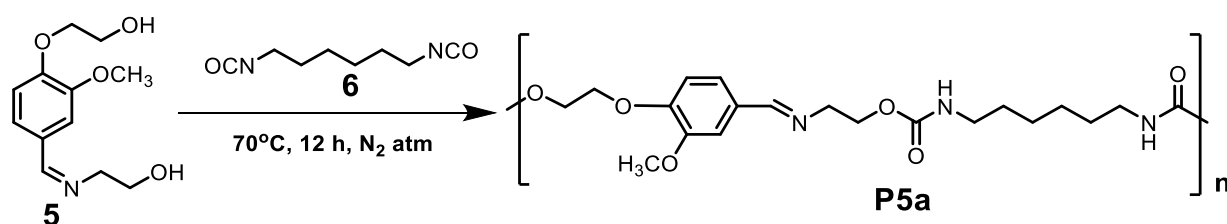
Scheme 3. Synthesis of monomer (7).

## 2.3 Polymer synthesis

### 2.3.1 Thermoplastics

#### Synthesis of Polyurethane (P5a)

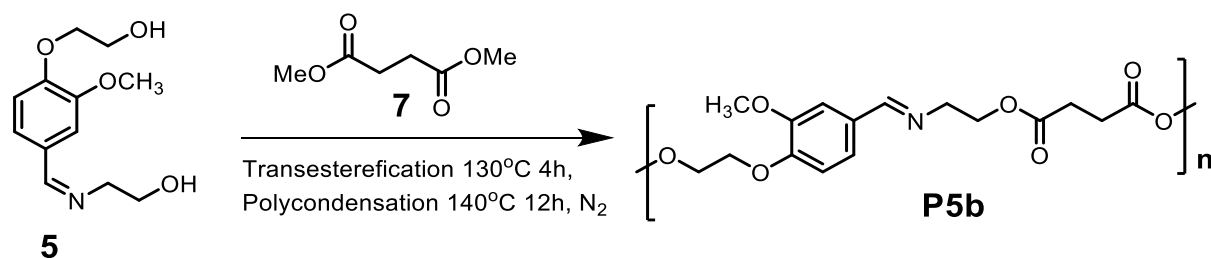
The synthesis of polyurethane was realized by using the monomer **5** react with hexamethylene diisocyanate in the presence of DBTDL as a catalyst and Ethyl acetate as a solvent. The solution was kept at 70°C for 12 h under N<sub>2</sub> atmosphere (Scheme 4). After the reaction, the precipitate was filtered, washed with ethyl acetate, and dried using vacuum oven for 12 h. The product is a white solid, and the yield is  $\geq 80\%$ .



Scheme 4. Synthesis of polyurethane (P5a).

#### Synthesis of Polyester (P5b)

The synthesis of polyester was realized by using monomer **5** and dimethyl succinate with DBTL as a catalyst and xylene as a solvent. The first step is the transesterification at 130°C for 4h under N<sub>2</sub> atm; it was monitored by <sup>1</sup>H NMR, then the second step is the polycondensation at 140°C for 12h under high N<sub>2</sub> flow (scheme 5). The product is then dissolved in DMSO and precipitated in EtOH.



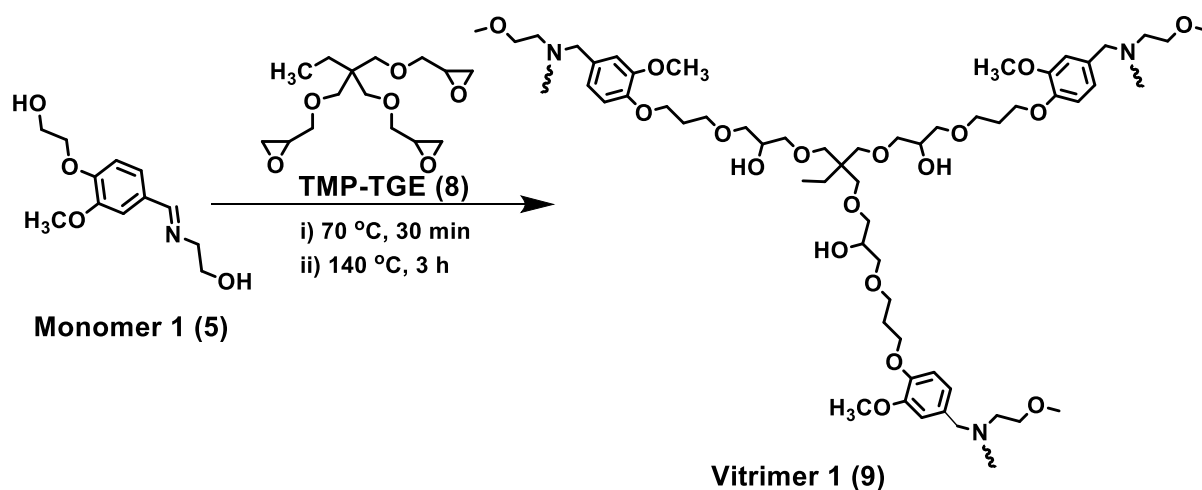
Scheme 5. Synthesis of polyester (P5b).

### 2.3.2 Vitrimers

#### Synthesis of Vitrimer 1 (9)

The reaction to synthesize the first type of Vitrimer involved the monomer 5 and trimethylolpropane triglycidyl ether (TMP-TGE) with ratio 1:1, with 1,2 dimetildimidazole as a catalyst. The reaction consists in dissolving the monomer, the reactant, and the catalyst in a vial at 70°C under stirring for 15 minutes.

When the solution is homogeneous is transferred to a Teflon mold that was previously heated at 140°C. After 4 hours, the Teflon mold is removed from the oven, and the reaction is stopped (Scheme 6). The result is a flexible material (figure 6).



Scheme 6. Synthesis of Vitrimer 1 (9).

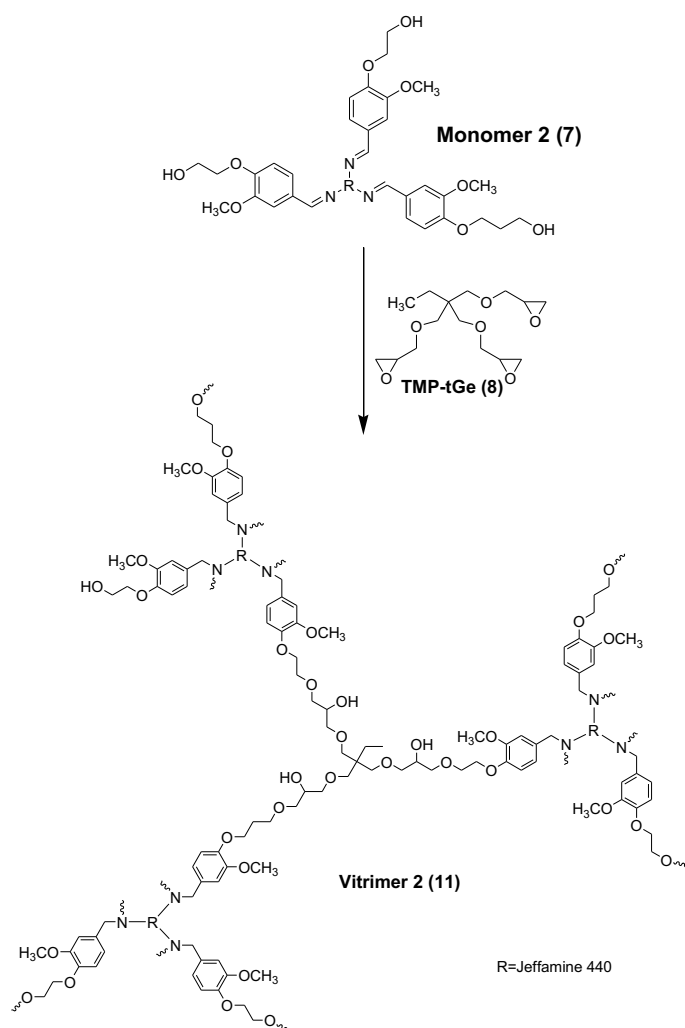


Figure 6. Vitrimer 1 (9) with different shapes.

### Synthesis of Vitrimer 2 (11)

The reaction to synthesize the second type of Vitrimer involved the monomer 7 and trimethylolpropane triglycidyl ether with ratio 1:1, with 1,2 dimetildimidazole as a catalyst. The reaction consists in dissolving the monomer with EtOH as a solvent, the reactant, and the catalyst in a vial at 70°C under stirring for 15 minutes.

When the solution is homogeneous is transferred into a Teflon mold that was previously heated at 140°C. After 4 hours the Teflon mold is removed from the oven, and the reaction is stopped (Scheme 7). The result is a flexible material (figure 8).



**Scheme 7. Synthesis of Vitrimer 2 (11).**



**Figure 7. Vitrimer 2 (11) with different shapes.**

## 2.4 Characterization methods

### 2.4.1 Qualitative analysis – ATR-FTIR, NMR, SEC analysis

#### ATR-FTIR

Attenuated total reflection – Fourier-transform infrared spectroscopy allows for qualifying samples without preparation in a solid or liquid state. An ATR accessory works by quantifying the variation that occurs to an internally-reflected IR beam when it comes in contact with the examined sample. The internal reflections create a transient wave that will be either altered or attenuated where the sample absorbs energy. Subsequently, the attenuated energy from the wave is led back to the original IR beam, which passes through the sample and goes to the detector. The instrument uses this information to create an IR spectrum [16,17].

The analysis was performed with a PerkinElmer 2000 spectrophotometer equipped with an attenuated total reflection (ATR) setup visible in figure 8. The sample was placed over the crucible of the instrument, then was covered with a pressure anvil which is tightened with the help of a screwdriver. The analysis is made in a range of 400 – 4000  $\text{cm}^{-1}$ .

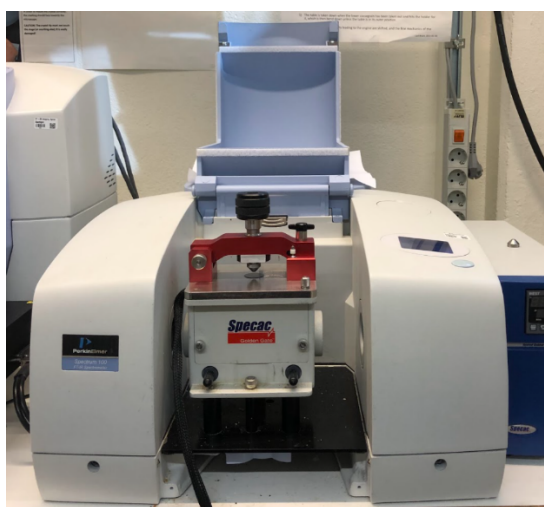


Figure 8. AT-FTIR instrument.

#### Nuclear Magnetic Resonance

Nuclear Magnetic Resonance (NMR) uses the difference of energy that spin states have in the presence of a magnetic field. It gives information about the structure of organic molecules.

The sensibility of this technique is relatively low because it depends on the difference of energy between the states and increases directly with the rise of the magnetic field

applied; furthermore, nuclei with a high gyromagnetic ratio are more sensible than nuclei with a low gyromagnetic ratio.

The most used nuclei are  $^1\text{H}$  and  $^{13}\text{C}$ . The proton has an isotopic abundance of 100% and the highest gyromagnetic ratio between the elements, while  $^{13}\text{C}$  has an isotopic abundance of 1,1% and  $\frac{1}{4}$  of the gyromagnetic ratio of  $^1\text{H}$ , but is the base element of the organic chemistry. In this work, both nuclei were used.

All protons are the same, but an electron cloud around a nucleus can shield the effect of the external magnetic field. It is, therefore, possible to relate the resonant frequency of the nuclei to the electron distribution in the molecule and consequently predict the chemical structure.

The external magnetic field induces a movement of the electrons in the electron cloud, which subsequently creates another magnetic field that opposes the external magnetic field inside the cloud and adds to the external magnetic field outside the cloud. The difference in the resonance frequency of nuclei in different chemical surroundings is called chemical shift.

The protons surrounded by high electronic density resonate to a lower frequency than compared with protons surrounded by low electronic density. For the analysis is not possible to measure just the resonance frequency of a proton in Hz, because it depends on the external magnetic field, which is not constant; small variations in the magnetic field could cause differences in the resonance frequency bigger than the chemical shift. For this reason, it is used as a reference substance, and dividing the difference between  $\nu$ -reference by resonant frequency is obtained an independent dimension, according to the formula:  $\delta = \frac{\nu - \nu_{reference}}{\nu} * 10^6$  [18].

The instrument used is an Avance 400 spectrometer at 298K (Figure 9). The samples were prepared by dissolving them in an NMR tube with deuterated DMSO, or  $\text{D}_2\text{O}$ . The chemical shifts were reported as  $\delta$  values (ppm) of the residual DMSO- $d_6$  (2.50 and 39.52 ppm) and  $\text{D}_2\text{O}$  (4.79 ppm) taken as a reference and the proton frequency of 400.13 MHz and a carbon frequency of 100.61 MHz respectively.



**Figure 9. NMR instrument.**

### *Size-exclusion chromatography*

Size-exclusion chromatography is a technique that classifies the molecule according to their size in a solution, exploiting a column filled with a porous rigid structure and porous particle column packing (stationary phase) and an eluent (mobile phase). The sample is dissolved in the eluent that rises through the column. Large molecules do not enter the pores, while small molecules flow through the pores of the column [19]. The smaller are the molecules, the faster is the diffusion through the column, giving a size separation as shown in figure 10.

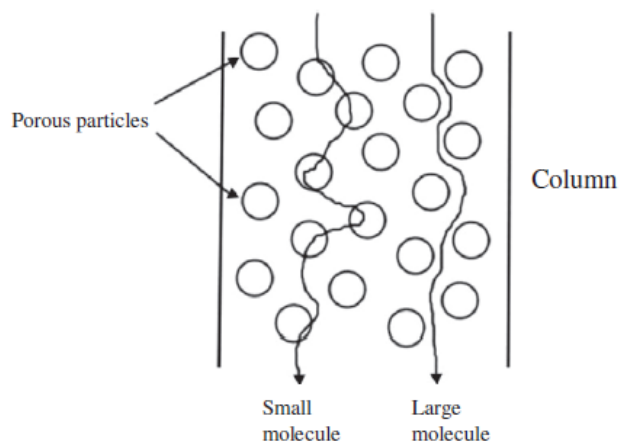


**Figure 10. Diffusion through the SEC column [19].**



The analysis was carried out with three PSS GRAM columns in series (KF-805, 2804, and 2802.5) and the system (Agilent Technologies 1260 Infinity, from PSS, Germany) equipped with a refractive index (RI) detector (G1362A 1260 RID Agilent Technologies) and a multi-angle laser light scattering (MALLS) detector (SLD 7000 PSS, Germany), (figure 11).

All the measurements were carried out at room temperature, DMSO and 0.5 wt% LiBr as eluent and the elution rate of 1 mL min<sup>-1</sup>. The system was calibrated with pullulan standards of narrow polydispersity (PSS, Germany). Polyesters were dissolved in SEC eluent and kept for 12 h. Afterward the polymer samples were filtered by using a membrane filters and transferred into special SEC vial and a volume of 100 µL of each sample were injected with the flow rate of 0.5 mL/min. Finally, the number and weight-average molecular weights (M<sub>n</sub> and M<sub>w</sub>) and polydispersity index were calculated with the WinGPC UniChrom GPC/SEC software (PSS, Germany) using light scattering calibration methods.



**Figure 11. SEC instrument.**

## 2.4.2 Thermal and mechanical properties -TGA, DSC, DMA analysis and tensile testing

### Thermogravimetric analysis

The main purpose of thermogravimetric analysis (TGA) is to determine the thermal stability of the sample. This can be done by measuring parameters like moisture loss, loss of solvent, oxidation, pyrolysis, weight % ash, and weight % filler.

This apparatus works by gauging the change in mass of the sample with the variation of the temperature or time in a controlled temperature. The machine consists of a pan that rests on a sensitive analytical balance. The sample is placed over the pan and is heated externally. The analysis can be carried out both in an inert atmosphere (with N<sub>2</sub> or Ar) and in an oxidizing atmosphere (presence of air). The heating rate is fixed and the mass variation is controlled continuously. A computer is connected to the apparatus to record the mass change and create the graph, that shows in abscissa (x-axis), time or temperature and in ordinate (y-axis) weight (mg) or percentage weight (%) [20]. A typical TGA graph is shown in figure 12.

The analysis were performed with a Mettler Toledo TGA 1 instrument (figure 13) at a heating rate of 10°C/min<sup>-1</sup> under nitrogen atmosphere with a purge rate of 50 mL min<sup>-1</sup> at 50°C – 600°C. The samples were kept isothermally at 150 °C for 15 min, to remove solvent residue. TGA data were analyzed by Mettler Toledo STARe v. 15.00 software.

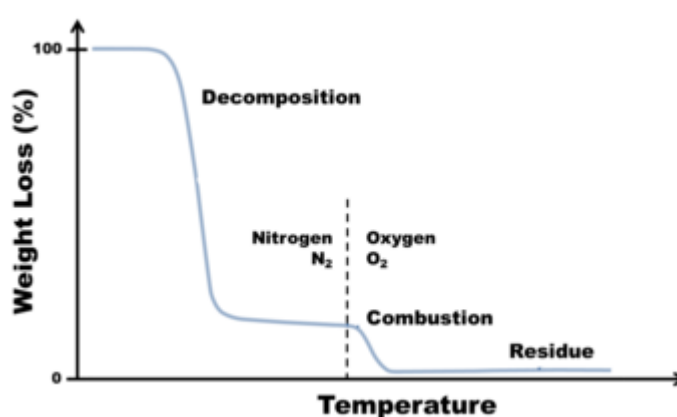


Figure 12. Typical TGA graph [21].



**Figure 13. TGA instrument.**

### *Differential scanning calorimeter*

The differential scanning calorimeter (DSC) allows determining the heat capacity, glass transition temperature, crystallization temperature, and melting point of a substance.

It consists of two solid pans resting on top of heaters. The sample being analysed is kept on one of the pans, and the other pan is kept empty as a reference. The rate of the temperature is controlled accurately and is recorded the amount of heat supplied to each pan. Usually, the amount of heat supplied to the reference pan is lower than with respect to the pan that contains the sample. The additional heat supplied to the sample is needed to maintain the same temperature rise as the reference sample.

During the analysis is built a graph, wherein the y-axis is plotted the difference in heat given out to maintain the identical temperature rise, while on the x-axis is plotted the temperature.

It is possible to determine the heat capacity  $C_p$ , which is constant until reaching glass transition temperature  $T_g$ . At this point, the sample requires more heat to raise the temperature.

Some molecules crystallize at a certain temperature, which can be determined by an exothermic peak in the plot since crystallization is an exothermic process.

Additional heating leads to melting, and this point ( $T_m$ ) is determined by an endothermic peak [22].

DSC measurements were performed using a Mettler Toledo DSC 1 instrument (figure 14). The samples were studied with a heating rate of  $10\text{ }^{\circ}\text{C min}^{-1}$  under nitrogen flow with a purge rate of  $50\text{ mL min}^{-1}$ . The sequence consisted of a heating ramp from  $-30$  to  $200\text{ }^{\circ}\text{C}$ , followed by a cooling ramp to  $0\text{ }^{\circ}\text{C}$  and finally a heating ramp to  $200\text{ }^{\circ}\text{C}$  and

the glass transition temperature ( $T_g$ ) was determined from second heating cycle. DSC data were analyzed by Mettler Toledo STARe v. 15.00 software.



**Figure 14. DSC instrument.**

### *Dynamic Mechanical Analysis*

Dynamic Mechanical Analysis (DMA) or Dynamic Mechanical Thermal Analysis (DMTA) is carried out by applying cyclic force (hence deformation) to a sample of known geometry and measuring the material's response to the stimuli. Response material is also observed during the variation of the temperature.

The sinusoidal deformation can be applied giving the sample a controlled strain or controlled stress. The amount of deformation is related to the stiffness 'material.

The instrument measures stiffness and damping, which are reported in a graph as modulus and tan delta. Since is applied a sinusoidal force, the modulus can be reported as an in-phase modulus and an out-phase modulus. The first modulus called storage modulus, known as  $E'$ , expresses the sample's elastic behaviour. The second one is called loss modulus, known as  $E''$ .

The ratio of the loss modulus to the storage is tan delta which can be also called damping. It gives information about the energy dissipation of the material under cyclic load. Tan delta measures the capacity of a material to dissipate energy. This quantity varies with the state of the material, its temperature and the applied frequency.

It is possible from DMA to detect  $T_g$ , since the materials tend to lose their modulus at this temperature. The  $T_g$  is then detected easily at the maximum point of the tan delta curve [23].

The analysis were performed using a TA Instruments Q800 in the tension film mode (figure 15). The samples were tested from  $-10$  to  $100$  °C at 1 Hz with a deflection of 0.5% strain and at a  $3^{\circ}\text{C}/\text{min}$  heating rate.



**Figure 15. DMA instrument.**

### *Tensile testing*

The tensile tests were performed by Instron 5944 universal testing machine (figure 16). The as synthesized samples had a uniform dimension of 80 mm x 4 mm x 1.2 mm, while the reprocessed samples had a dimension of 20 mm x 4 mm x 0.7 mm. All the samples were conditioned at  $22^{\circ}\text{C}$  and 40% of relative humidity for two days before testing.



**Figure 16. Tensile test instrument.**





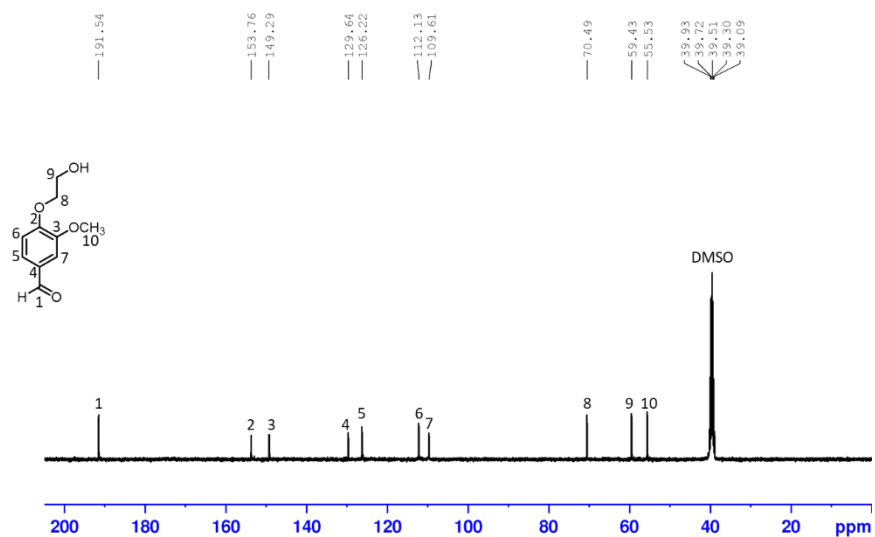


Figure 18. <sup>13</sup>C NMR (100.61 MHz, DMSO-*d*<sub>6</sub>) spectrum of compound (3).

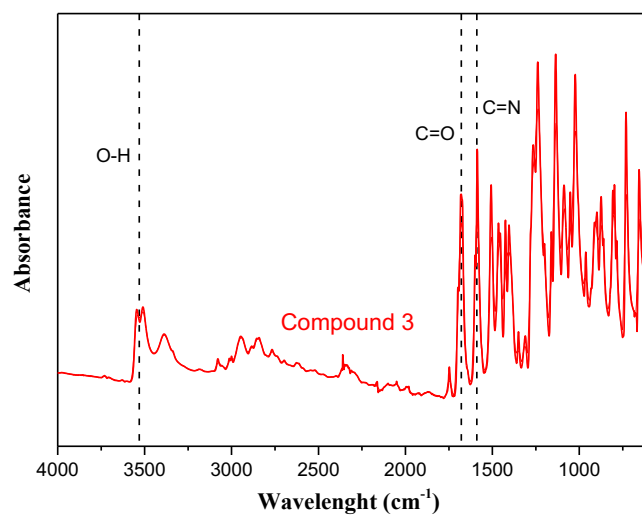
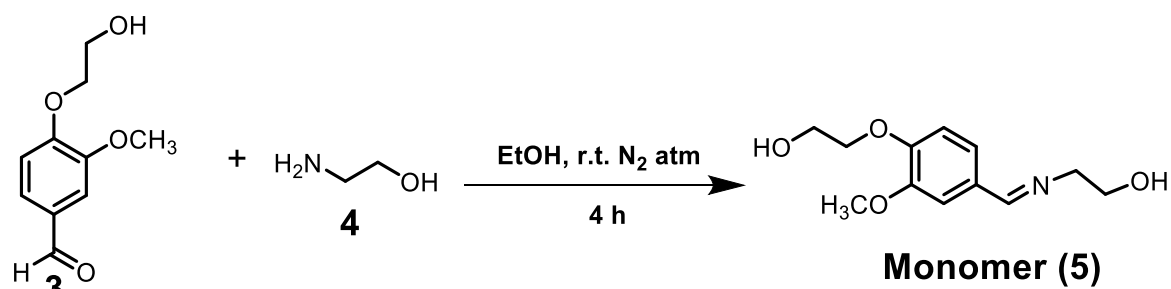


Figure 19. FTIR of compound (3).



## Synthesis of monomer 1 (5)



**Scheme 2. Synthesis of monomer 1 (5).**

The monomer (5) was characterised to monitor that the reaction had occurred. The  $^1\text{H}$  NMR analysis (Figure 20),  $^{13}\text{C}$  NMR analysis (Figure 21), and FTIR analysis (Figure 22) have been conducted on the synthesized monomer confirm the chemical structure.

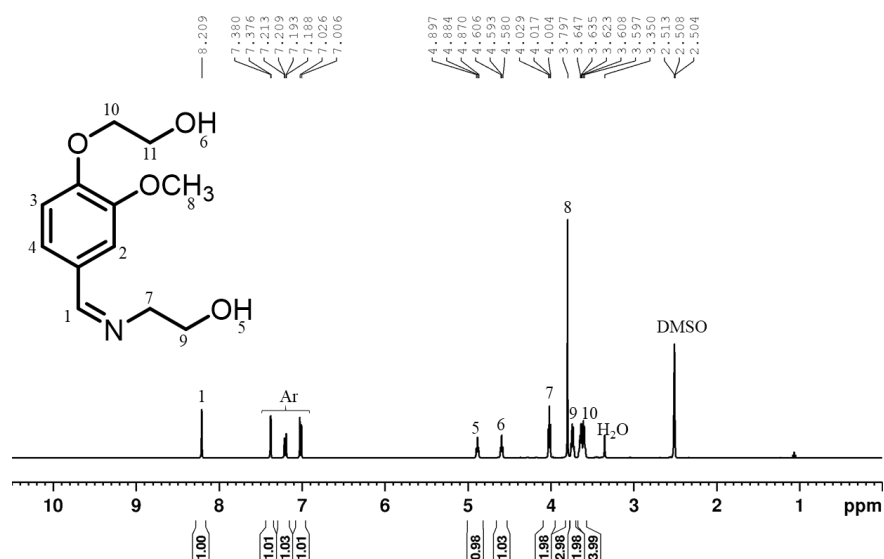


**Figure 20.  $^1\text{H}$  NMR (400.13 MHz, DMSO- $d_6$ ) spectrum of monomer 1 (5).**

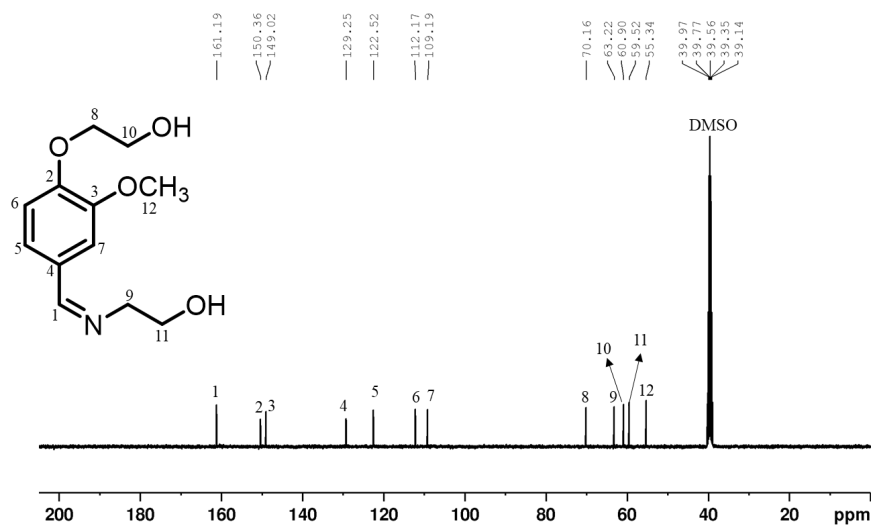


**Figure 21.  $^{13}\text{C}$  NMR (100.61 MHz, DMSO- $d_6$ ) spectrum of monomer 1 (5).**

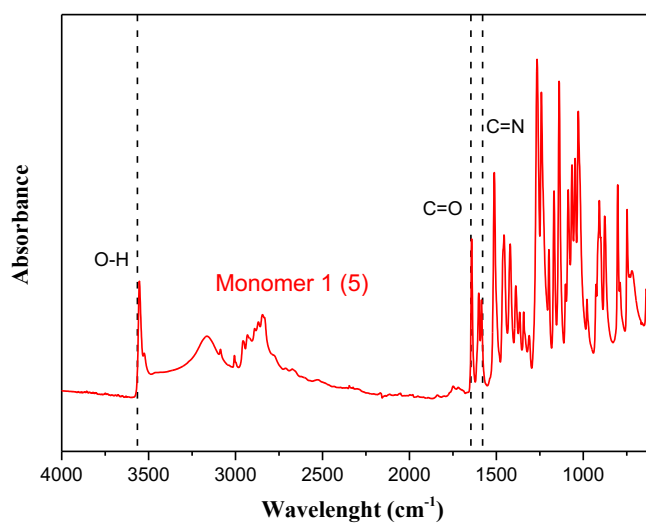


**Figure 22. FTIR of monomer 1 (5).**

### *TGA analysis*

The TGA analysis was carried out with a temperature range between 30°C and 600°C in an inert atmosphere. The analysis in figure 23 shows a residue of 31.7% and good thermal stability, since the temperature at which the sample begins to lose weight is around 150°C, and the temperature at which the monomer has the maximum weight loss is around 300°C.

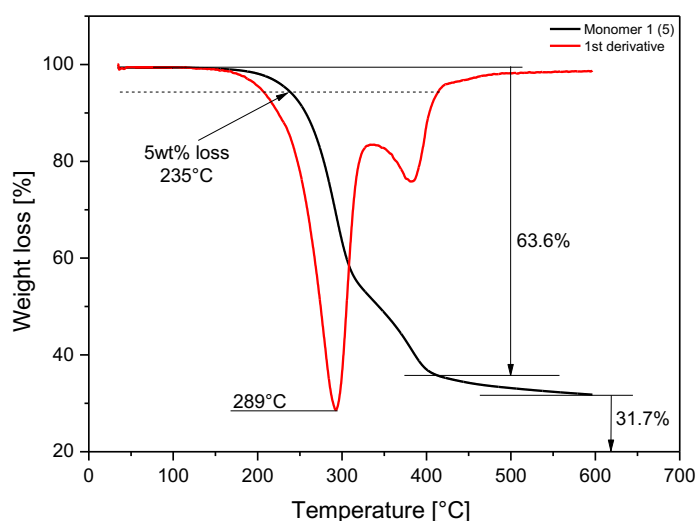
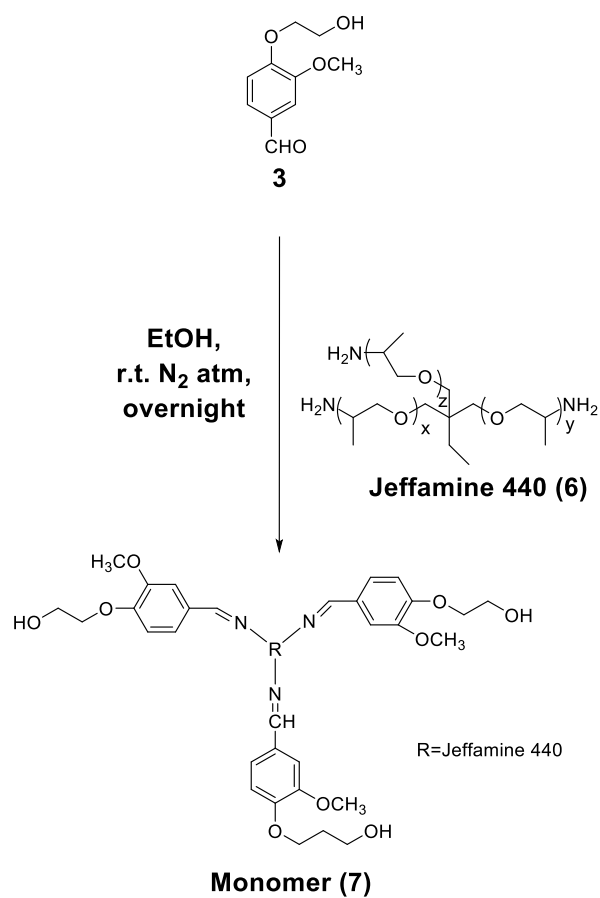


**Figure 23. TGA of monomer 1 (5).**

## Synthesis of monomer 2 (7)



**Scheme 2. Synthesis of monomer 2 (7).**

Monomer (7) was characterised. The  $^1\text{H}$  NMR analysis (Figure 24), and FTIR analysis (Figure 25) were conducted.

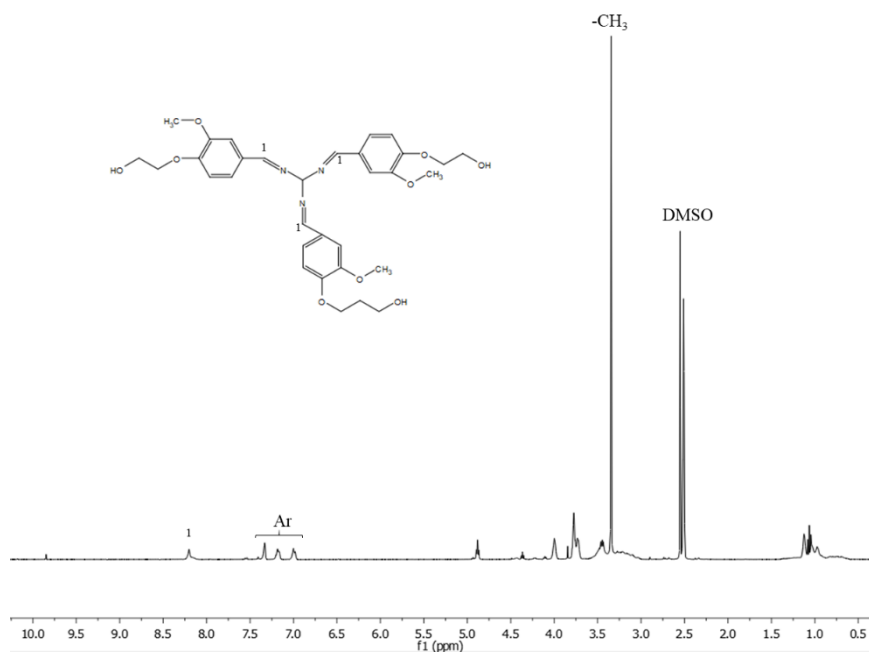


**Figure 24.  $^1\text{H}$  NMR (400.13 MHz, DMSO- $d_6$ ) spectrum of monomer 2 (7).**

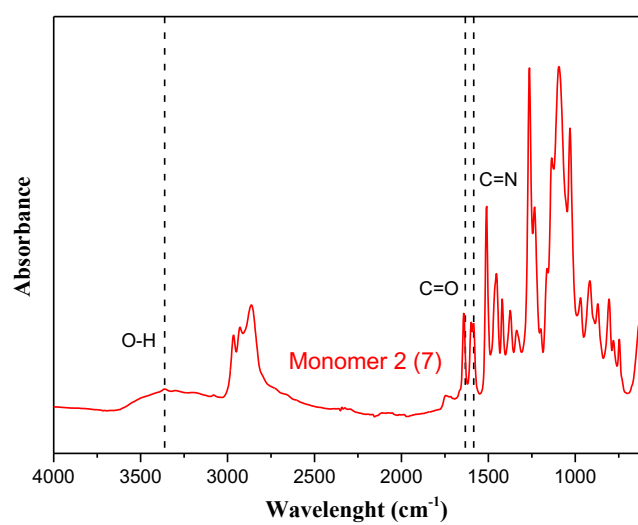


**Figure 25. FTIR of monomer 2 (7).**

### *TGA analysis*

The TGA analysis was carried out with a temperature range between 30°C and 600°C in an inert atmosphere. The analysis in figure 26 shows a residue of 17.5% and good thermal stability, since the temperature at which the sample begins to lose weight is around 200°C, and the temperature at which the sample has the maximum weight loss is around 350°C.

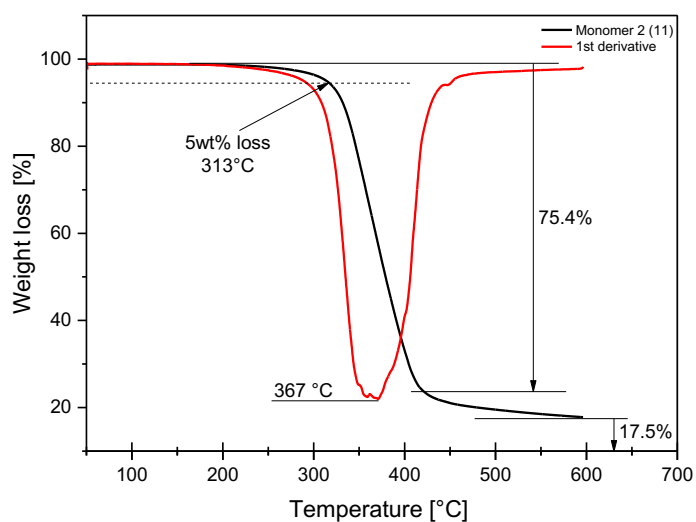
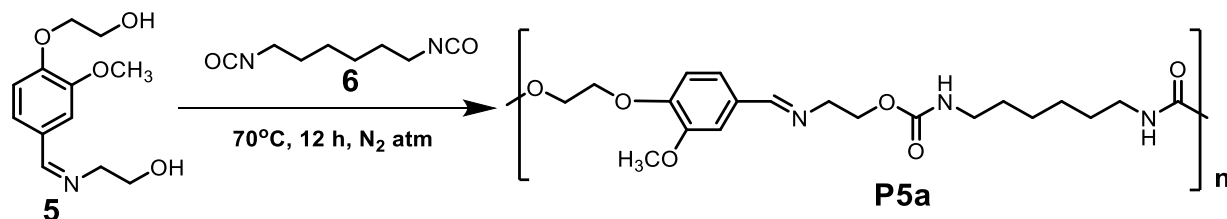


**Figure 26. TGA of monomer 2 (7).**

## 3.2 Thermoplastic polymers synthesis

### 3.2.1 Synthesis of Polyurethane (P5a)



Scheme 4. Synthesis of polyurethane (P5a).

The synthesized diol (compound 5) was reacted with isocyanate (compound 6). After the synthesis of the polyurethane, the product has been characterized to confirm that the reaction had occurred by <sup>1</sup>H NMR analysis (Figure 27) and FTIR analysis (Figure 28). The FTIR analysis has been compared with the FTIR spectra of the precursors of the polymer to show that the -OH of the initial monomer (5) peak disappeared and to show that are appeared the -NH peak and the C=O peak, that belongs of the polyurethane (P5a).

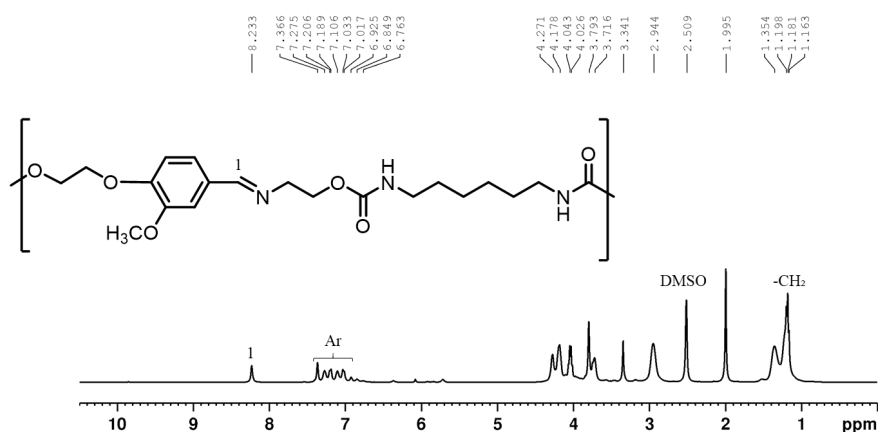
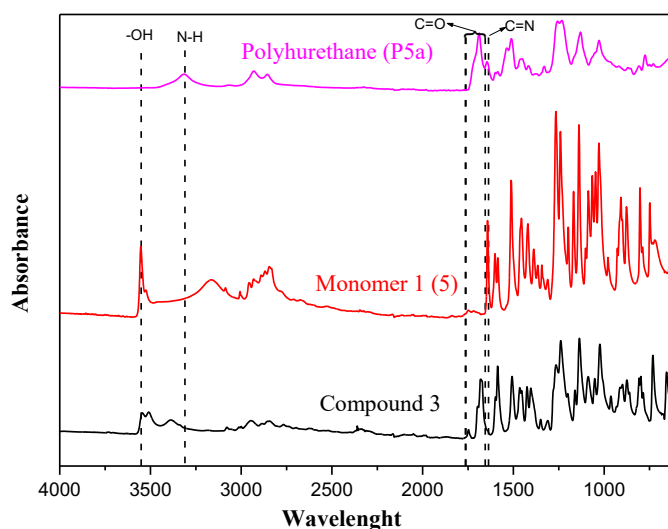


Figure 27. <sup>1</sup>H NMR (400.13 MHz, DMSO-*d*<sub>6</sub>) spectrum of polyurethane (P5a).



**Figure 28. Comparison of polyurethane (P5a) FTIR spectra with monomer and precursor.**

#### *SEC analysis*

SEC analysis was performed (figure 29) on the synthesized polymer. From the analysis, it is determined Number of average molecular weight ( $M_n$ ), Weight average molecular weight ( $M_w$ ), and the resultant Polydispersity index ( $D$ ), visible in table 1. The average molecular weight from the analysis results above  $10\,000\text{ g mol}^{-1}$ , value that is comparable with the conventional polyurethanes polymers reported in literature [24,25].

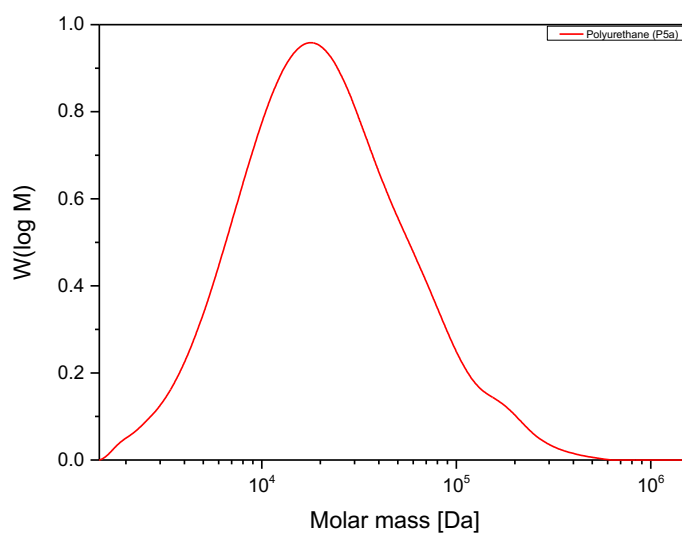


**Figure 29. SEC of polyurethane (P5a).**

$M_n$ (g mol <sup>-1</sup> )	$M_w$ (g mol <sup>-1</sup> )	<b>D</b>
13 400	34 600	2.59

**Table 1. Resulting value from SEC analysis.**

### *DSC analysis*

The DSC analysis was carried out with a temperature ramp with a range between -30 and 200°C. Analysing the DSC curve in figure 30, that represent the second heating, it is possible to determine the temperature of glass transition  $T_g$  of 55°C.

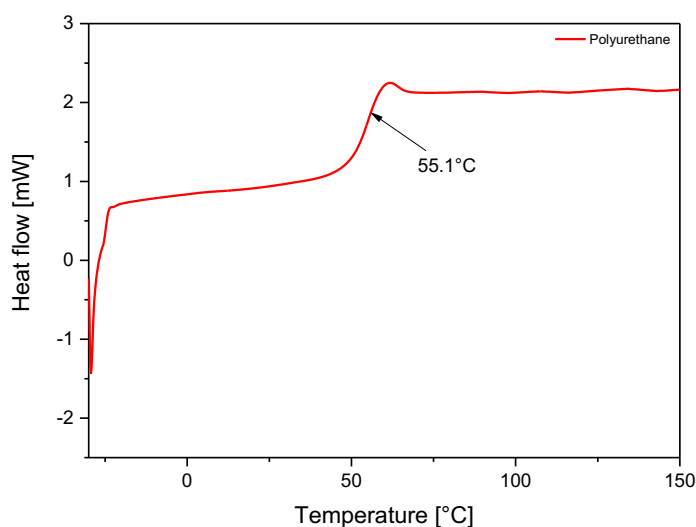


**Figure 30. DSC of polyurethane (P5a).**

### *TGA analysis*

The TGA analysis was carried out with a temperature range between 30°C and 600°C in an inert atmosphere. The analysis in figure 31 shows a residue of 11.5% and good thermal stability since the temperature at which the sample begins to lose weight is around 250°C, and the temperature at which the sample has the maximum weight loss ratio is around 300°C.

It is visible from the curve that there are three steps of degradation that can derive from the breaking at different times of the bonds. The first degradation step probably corresponds to the breaking of the imine bond, the second to the urethane bond, and the



third to the ether or ester bond. In order to confirm this theory, more studies would be required.

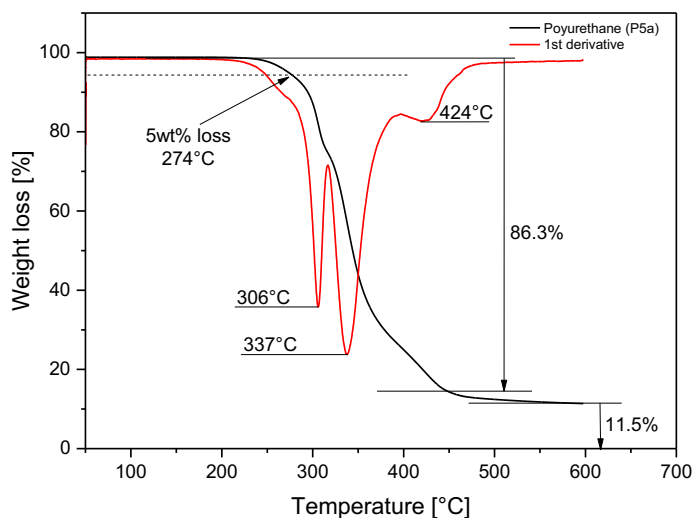


**Figure 31. TGA of Polyurethane (P5a).**

### *Chemical recycling*

It has been tested the chemical recycling of the synthesized polyurethane. The test involved 50 mg immersed in a solution of D<sub>2</sub>O HCl 0.1M, contained in an NMR tube. It has been monitored the <sup>1</sup>H NMR spectra of the solution over time.

From Figure 32, it can be observed that after 5 mins, it appears the -NH peak typical of polyurethane. The intensity of the peak is low because the polyurethane was not completely dissolved in the acidic solution after 5 minutes. Following the spectra, is noticeable that the -NH peak disappear because the polyurethane is degraded, while the peaks of the monomer (5), such as -CHO, appears, demonstrating that is possible to degrade the polymer in acid condition.

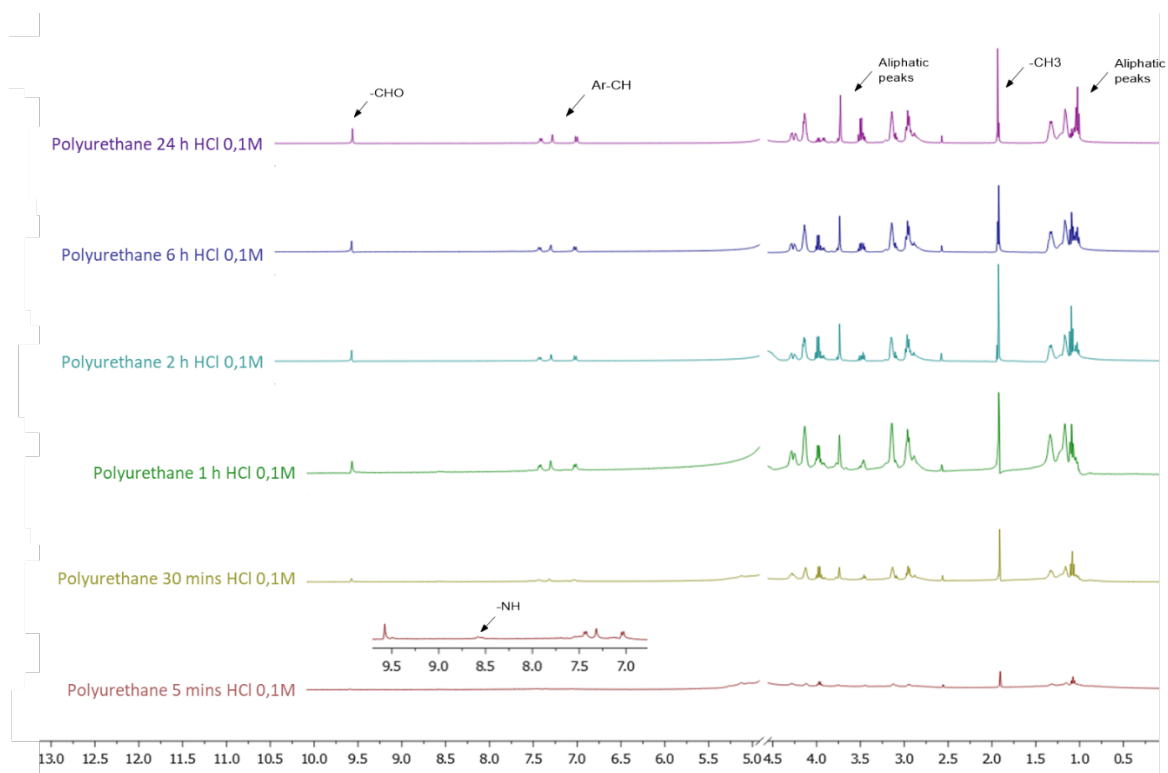
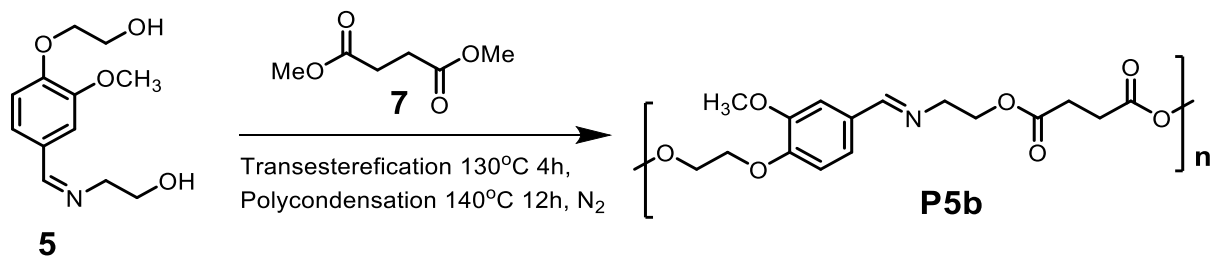


**Figure 32.** Comparison of NMR spectra of Polyurethane (P5a) in HCl 0.1M during time.

### 3.2.2 Synthesis of Polyester (P5b)



Scheme 5. Synthesis of polyester (P5b).

The same synthesized diol (compound 5) was reacted with a diester (compound 7). After the synthesis of the polyester, the product has been characterized to confirm that the reaction had occurred by  $^1\text{H}$  NMR analysis (Figure 33) and FTIR analysis (Figure 34). The FTIR analysis has been compared with the FTIR spectra of the precursors of the polymer (figure 32) to show that the -OH of the initial monomer (5) peak disappeared and to show that have appeared the C=O peak and the C=N peak, typical of the polyester (P5b).

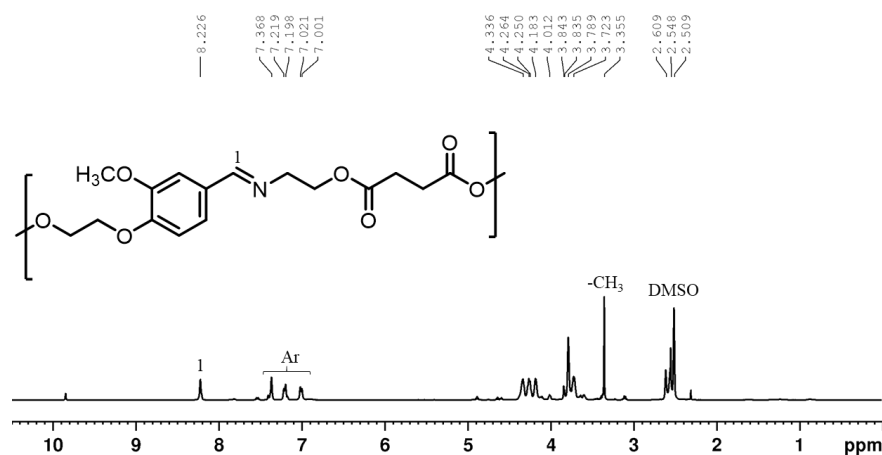
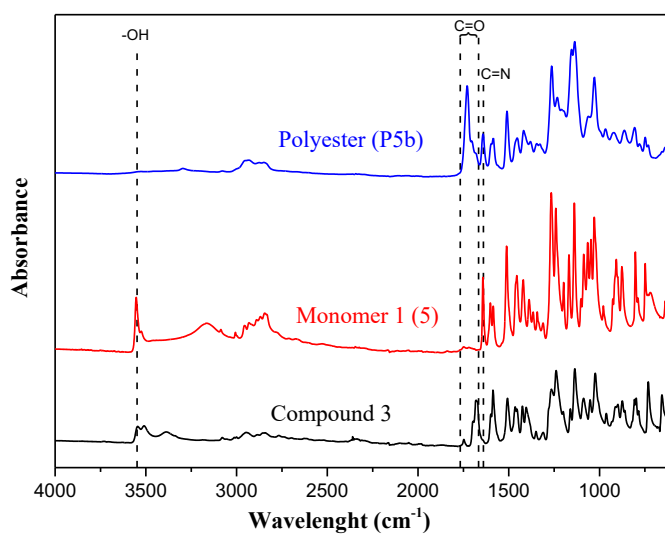


Figure 33.  $^1\text{H}$  NMR (400.13 MHz, DMSO- $d_6$ ) spectrum of polyester (P5b).



**Figure 34. Comparison of polyester (P5b) spectra with monomer and precursor.**

#### *TGA analysis*

The TGA analysis was carried out with a temperature range between 30°C and 600°C in an inert atmosphere. The analysis in figure 35 shows a residue of 29.9% and good thermal stability since the temperature at which the sample begins to lose weight is around 200°C, and the temperature at which the sample has the maximum weight loss ratio is around 300°C.

It is visible from the curve that there are two steps of degradation that can derive from the breaking at different times of the bonds. The first degradation step probably corresponds to the breaking of the imine bond, the second to the ether or ester bond. In order to confirm this theory, more studies would be required.

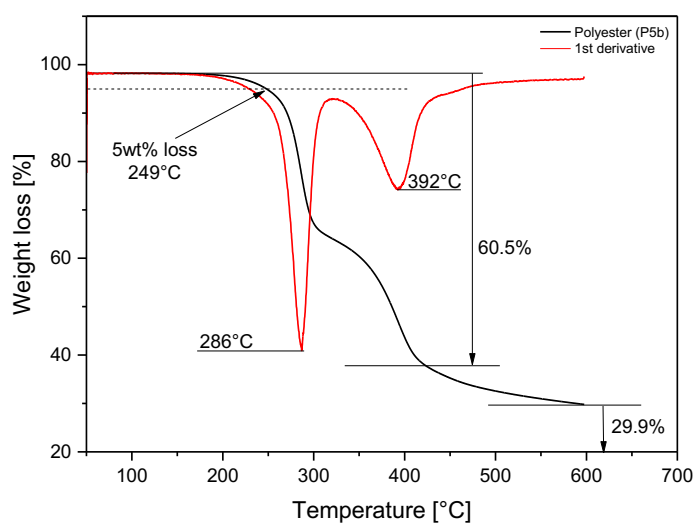


**Figure 35. TGA of Polyester (P5b)**

### *SEC analysis*

To characterize the polymer, it has been made a SEC analysis (figure 36). From the analysis, it is determined Number of average molecular weight ( $M_n$ ) and Weight average molecular weight ( $M_w$ ), represented in Table 2. The average molecular weight from the analysis results above  $10\,000\text{ g mol}^{-1}$ , value that is comparable with the conventional polyester polymers [26,27].

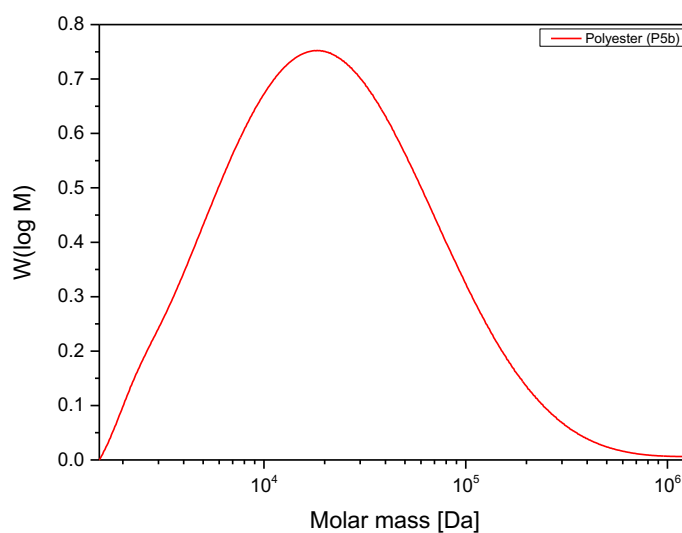


**Figure 36. SEC of polyester (P5b).**

$M_n$ (g mol <sup>-1</sup> )	$M_w$ (g mol <sup>-1</sup> )	<b>D</b>
11 750	42 890	3.64

**Table 2. Resulting value from SEC analysis.**

### *DSC analysis*

The DSC analysis was carried out with a temperature ramp with a range between -30 and 200°C. Analysing the DSC curve in Figure 37, which represent the second heating, it is possible to determine the temperature of glass transition  $T_g$  of 29°C. The  $T_g$  value is lower than the polyurethane (P5a) because the polyurethane has a major rigidity conferred by -NHCOO linkages. From the SEC analysis is also known that the polyurethane (P5a) has a higher molecular weight ( $M_n$ ), that increase the glass transition temperature.

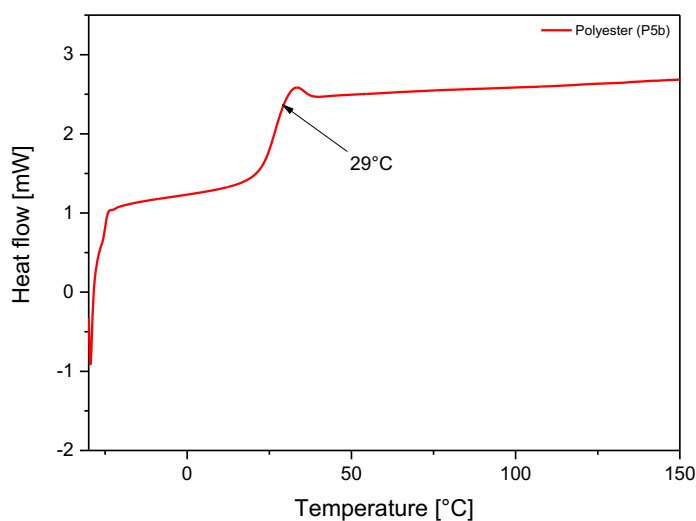
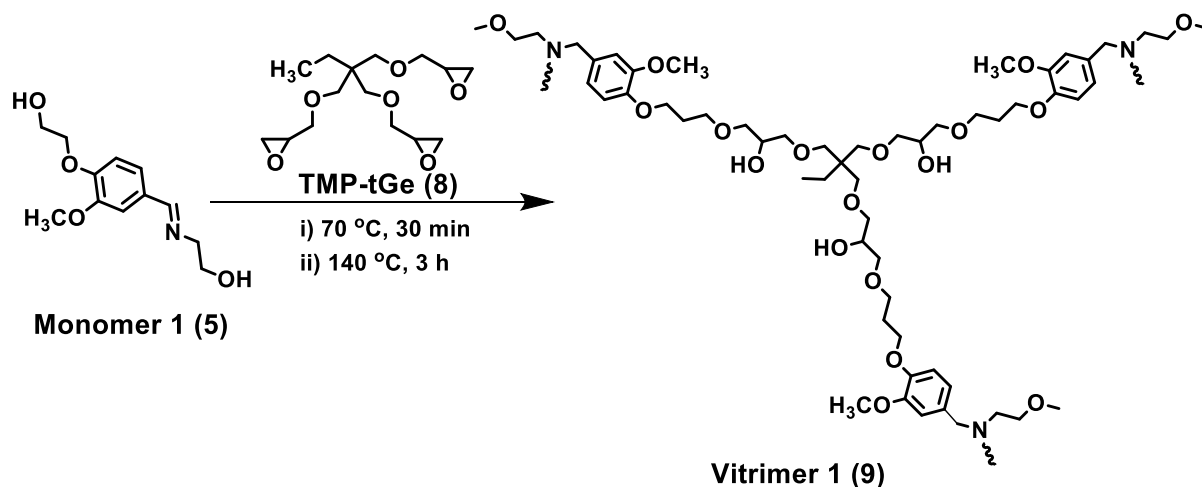


**Figure 37. DSC of polyester (P5b).**

### 3.3 Thermoset polymers synthesis - vitrimers

#### 3.3.1 Synthesis of Vitrimer 1 (9)



Scheme 6. Synthesis of Vitrimer 1 (9).

#### FTIR analysis

The synthesized diol (compound 5) was used to achieve a Vitrimer by reacting with a triglycidyl epoxy monomer. The reaction was followed by FTIR analysis (Figure 38), that shows a disappearance of the primary -OH peak and the appearance of the secondary -OH peak, giving the confirmation that the terminal -OH of the initial monomer are reacted to form the final structure. Furthermore, the intensity of C=N bond decreased since in the final structure is reacted to form crosslinks.

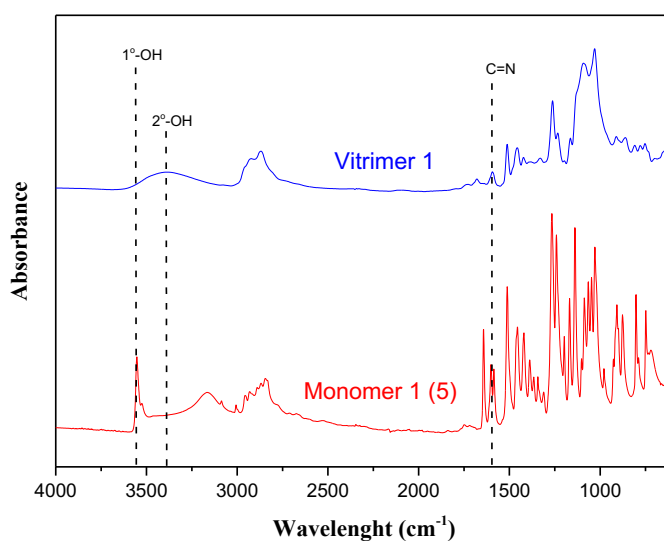
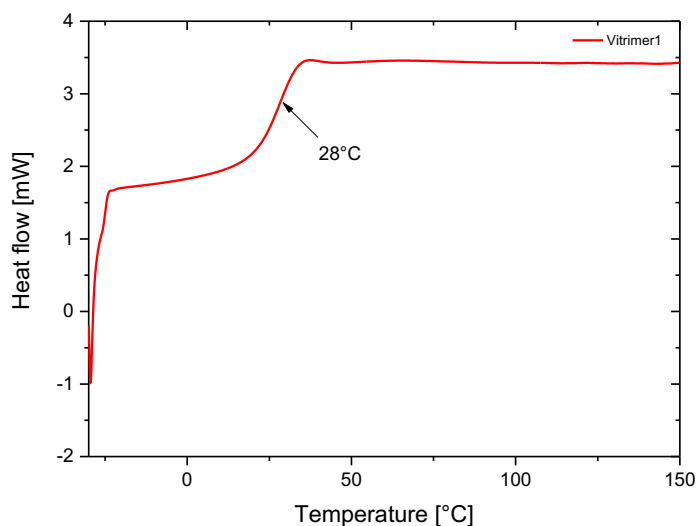


Figure 38. Comparison of Vitrimer 1 FTIR spectra with monomer 1 (5).

### *DSC analysis*

The DSC analysis was carried out on crosslinked polymer with a temperature ramp with a range between -30 and 200°C. Analysing the DSC curve in figure 39, that represent the second heating, it is possible to determine the temperature of glass transition  $T_g$  of 28°C.



**Figure 39. DSC of Vitrimers 1 (9)**

### *TGA analysis*

The TGA analysis was carried out with a temperature range between 30°C and 600°C in an inert atmosphere. The analysis in figure 40 shows a residue of 28.6% and good thermal stability, since the temperature at which the sample begins to lose weight is around 250°C, and the temperature at which the sample has the maximum weight loss is around 350°C. In the curve are present two degradation steps. The first degradation step could be due to the unreacted monomer that degrades before the Vitrimers since the temperature



at which is visible the first peak is close to the temperature of maximum degradation of monomer 1 (5) (Figure 23).

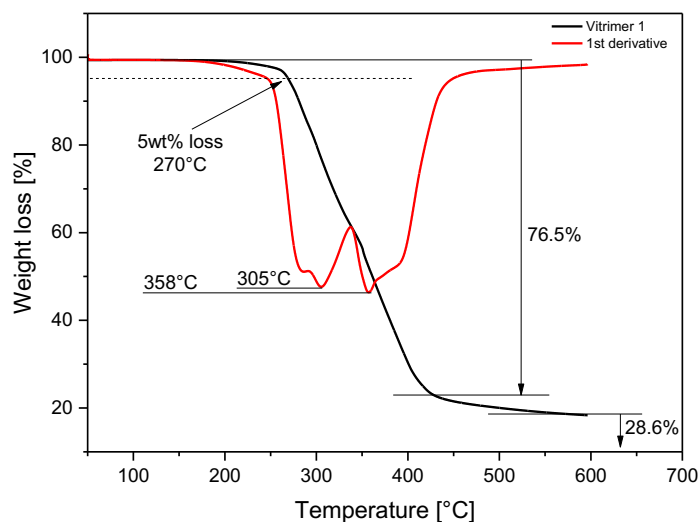


**Figure 40. TGA of Vitrimer 1 (9)**

### *DMA analysis*

The DMA analysis was carried out with a temperature range between -10°C and 100°C. From the analysis, shown in figure 41, it is possible to notice the temperature of glass transition at 36°C and the storage modulus ( $E'$ ) at 10°C of 1456.23 MPa. Furthermore, the storage modulus above  $T_g$  at 80°C correspond to 2.58 MPa.

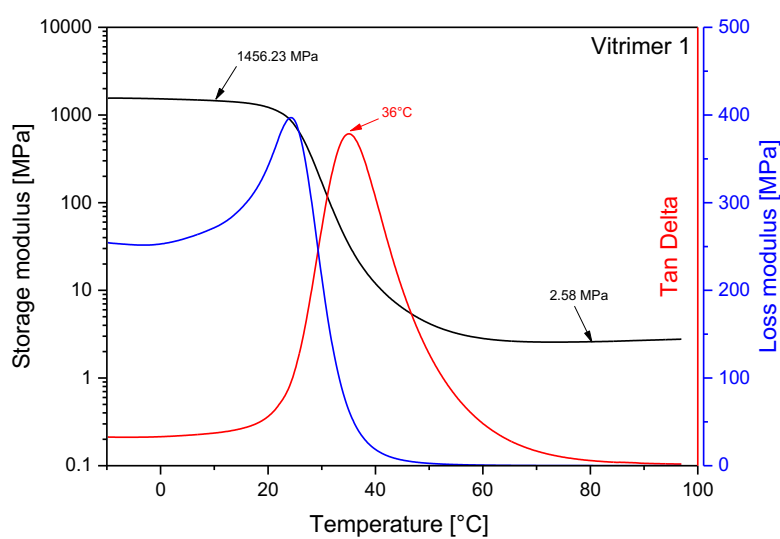


**Figure 41. DMA of Vitrimer 1 (9)**

### *Tensile test*

The tensile tests of the Vitrimer 1 (9) involved 4 different samples. In figure 42 is reported one test as a representative curve. In table 3 are reported the average values of elastic modulus (expressed in MPa), extension at break (expressed as a percentage) and tensile stress break (MPa). It has to be notified a high values dispersion, that can be derived from the fabrication method of the sample. During the pouring of the viscous solution in the Teflon mould some air bubbles can be entrapped, causing an early breaking of the sample.

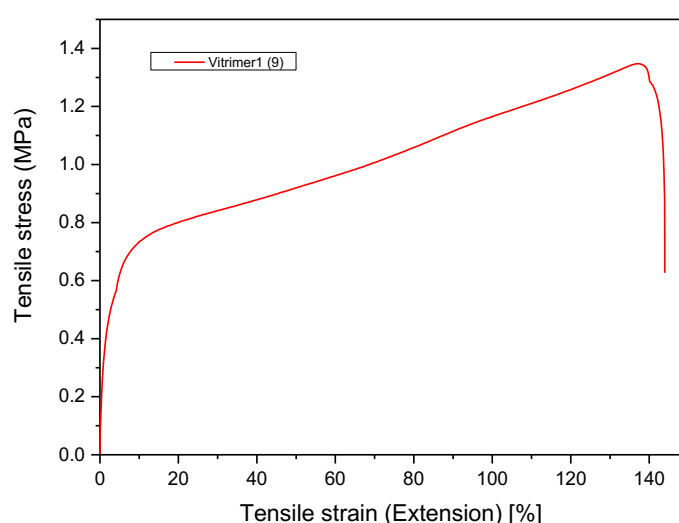


**Figure 42. Tensile test of Vitrimer 1 (9)**

Sample	Elastic modulus (MPa)	Tensile stress at break (MPa)	Extension at break (%)
Vitrimer 1 (9)	11.97±1.65	1.20±0.12 MPa	139.31±6.94

**Table 3. Tensile test of Vitrimer 1 (9)**

### *Mixture conversion*

In order to evaluate the amount of conversion of the precursors of Vitrimer 1 (9), it has been made a study following the DSC of the reaction mixture. First, it has been made a dynamic-DSC analysis of the reaction mixture of Vitrimer 1 (9) (red curve in Figure 43). From this analysis, it has been calculated the integral of the peak that corresponds to the enthalpy of 100% epoxy group conversion. The peak of the curve is at 119°C, and for this reason, an isothermal DSC of the mixture was carried out at 119°C for 180 minutes (blue curve in Figure 43). In this case, the integral of the isothermal DSC, that correspond

to the reaction enthalpy at 119°C, showed an enthalpy of -292 mJ, which divided by the integral's peak of 100% enthalpy (-689 mJ), gives 42% of conversion of the initial mixture.

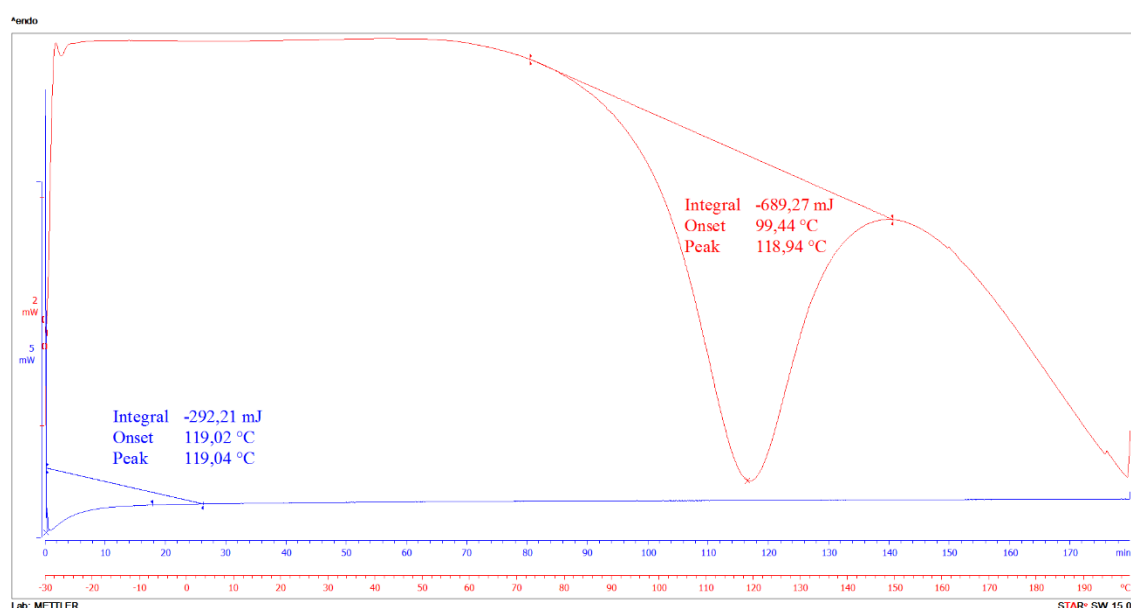


**Figure 43.** DSC of reaction mixture (red curve) and isothermal DSC of reaction mixture (blue curve).

### *Gel content test*

The gel content test was carried out with two different solvents, ethanol (EtOH) and tetrahydrofuran (THF), that solubilise the starting monomer. As visible in the table 4, the average gel content of Vitrimer 1 (9) after three days in both cases is around 94%. As visible in the Figures 44 and 45, the polymer was not dissolved at the end of the test.

Sample	Average gel content (%) in EtOH	Average gel content (%) in THF
Vitrimer 1 (9)	94.8±0.6	93.7±0.6

**Table 4.** Gel content test of Vitrimer 1 (9).

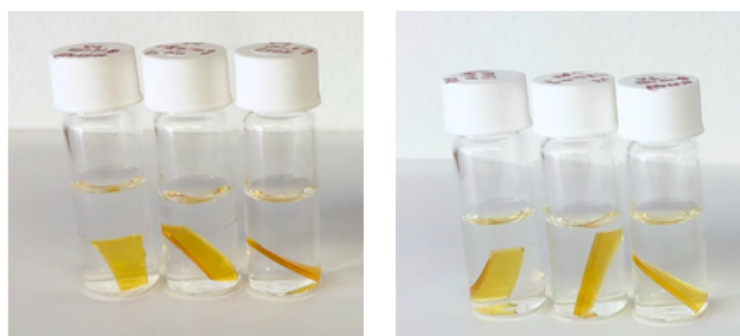


**Figure 44.** Vitrimer 1 in EtOH, start and after three days.

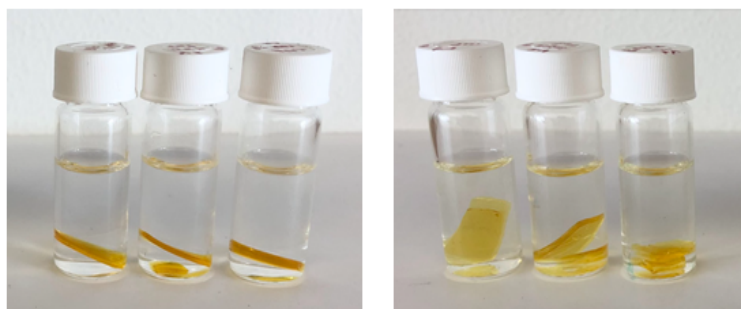


**Figure 45. Vitrimer 1 in THF, start and after three days.**

### *Chemical resistance*

Seven sample of Vitrimer 1 (9) were placed in seven different vials containing solvents and the chemical resistance was tested. The samples weighted 50 mg, and the solvents were acetone, tetrahydrofuran (THF), dimethylformamide (DMF), dicloromethane (DCM), sodium hydroxide (NaOH) 1M, ethanol (EtOH) and dimethyl sulfoxide (DMSO). After two days the Vitrimer dissolved partially only in DMSO and DMF, showing an excellent chemical resistance in the most common solvents (Figure 46).

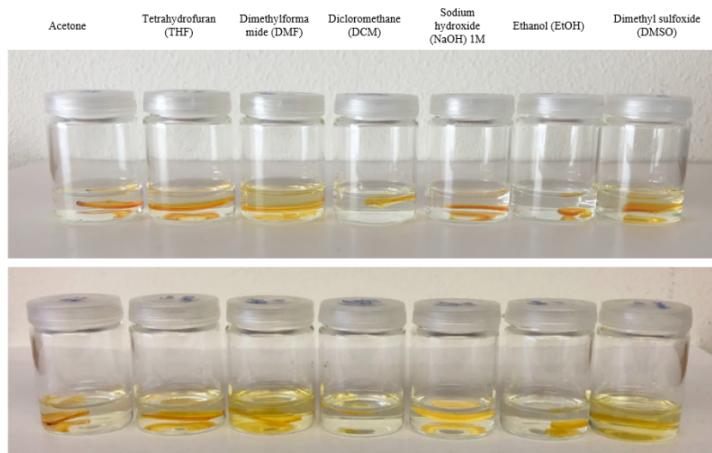


**Figure 46. Chemical resistance test, start and after 2 days.**

### *Chemical recycling*

Degradation tests were performed with the aim of demonstrating that the structure of the synthesized Vitrimer 1 (9) can be easily broken to form the starting materials again. Before following the degradation of the polymer in acidic conditions with  $^1\text{H}$  NMR, 50 mg of the polymer was placed in a vial filled with 2 ml of hydrochloric acid (HCl) 1M. The Vitrimer was fully dissolved in the solution in less than one hour, demonstrating that the imine bond is readily broken under acidic conditions.

Once proved the degradation in strong acid condition, the same test was conducted again in a less concentrated solution of hydrochloric acid (HCl) 0.1M (Figure 47). The Vitrimer, in these conditions, was entirely dissolved in two hours, and the entire process was followed by  $^1\text{H}$  NMR (Figure 48). Following NMR spectra during the time, it is noticeable that the -CHO peak, which belongs to monomer 1 (5), has increased the intensity after two hours. From this information, it is deduced that the polymer is dissolved in the starting material.

In order to show the formation of the starting materials after the dissolution, it has been compared  $^1\text{H}$  NMR of Vitrimer 1 (9) after two hours in acid condition with the starting materials (Figure 49). In the spectra are visible the main peaks that belong to the precursors of the polymer.

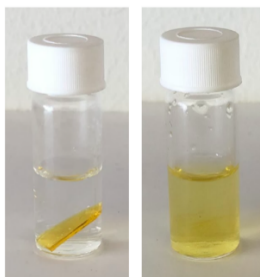


**Figure 47. Vitrimer 1 (9) in HCl 0.1M start and after 2h.**

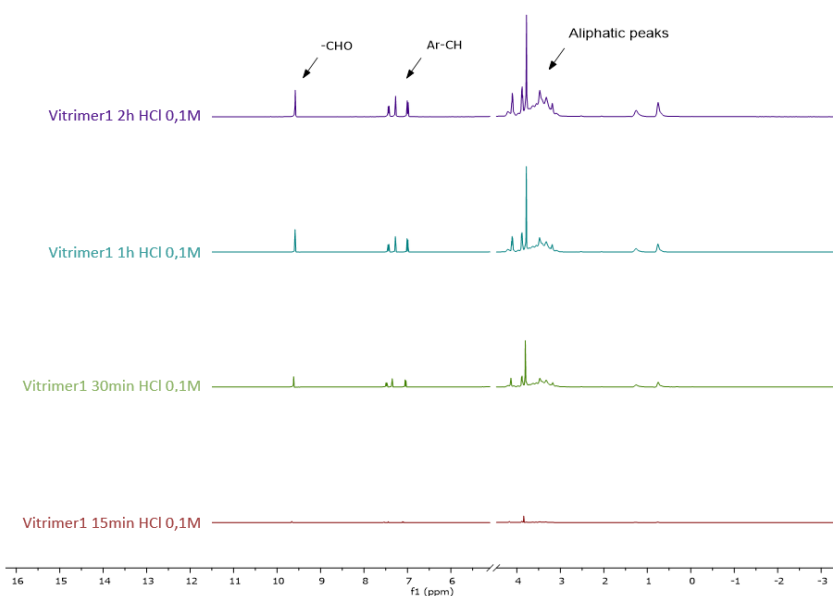


**Figure 48. Comparison of NMR spectra of Vitrimer 1 (9) in HCl 0.1 M during time.**

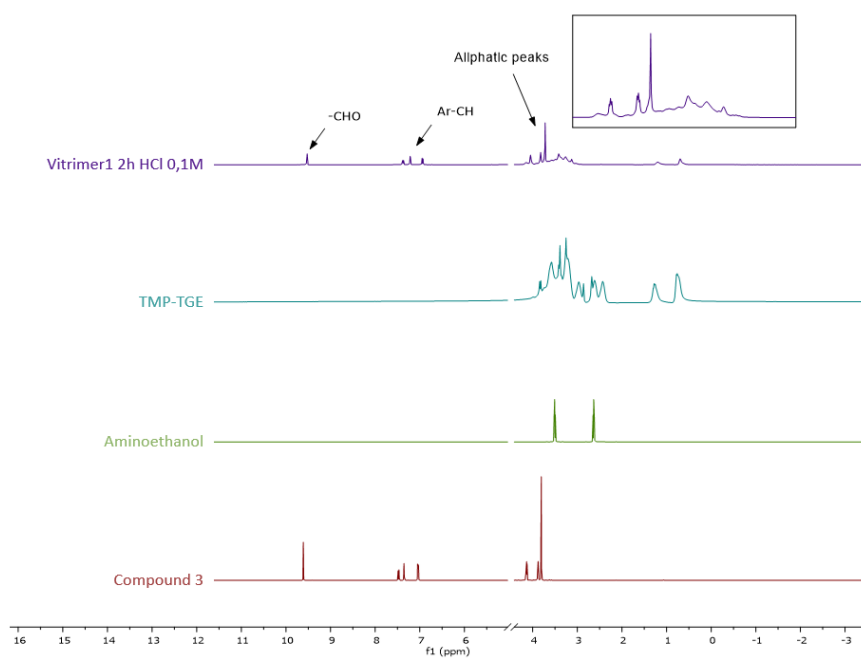
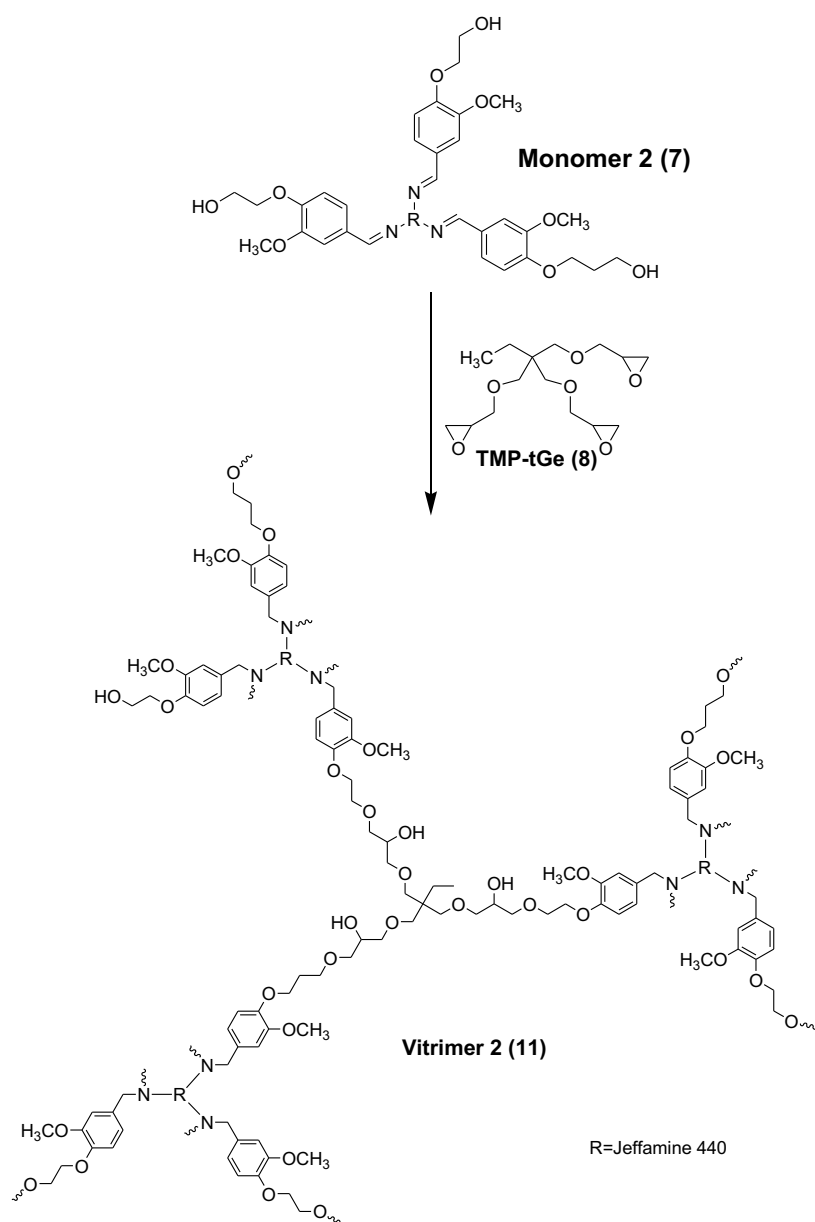


**Figure 49. Comparison of  $^1\text{H}$  NMR spectra of Vitrimer 1 (9) after 2h in HCl 0.1 with precursors.**

### 3.3.2 Synthesis of Vitrimer 2 (11)



**Scheme 7. Synthesis of Vitrimer 2 (11).**

Vitrimer 2 (11), achieved from monomer 2 reacting with the same triglycidil epoxy monomer, has been characterized following the same method of Vitrimer 1 (9). Like in

the previous case, the FTIR analysis is compared with the precursor of the Vitrimer 2 (11), in order to show the increment of the secondary -OH peak (Figure 50).

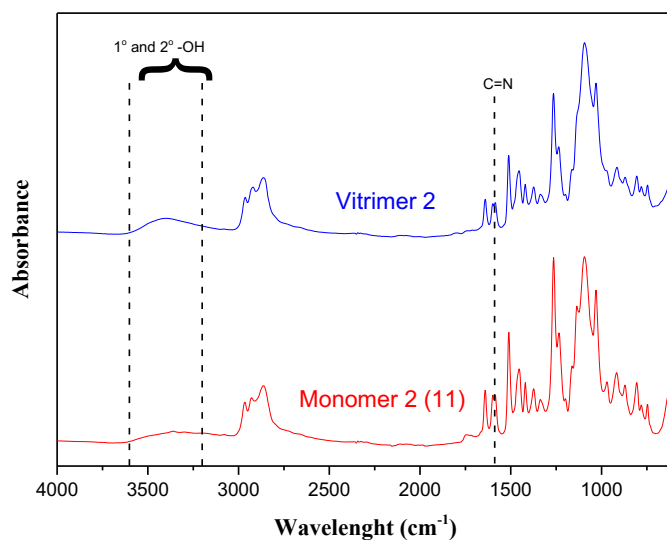


**Figure 50. Comparison of Vitrimer 2 (11) FTIR spectra with monomer 2 (7).**

#### *DSC analysis*

The DSC analysis was carried out with a temperature ramp with a range between -30 and 200°C. Analysing the DSC curve in Figure 51, that represent the second heating, it is possible to determine the temperature of glass transition  $T_g$  of 29°C.

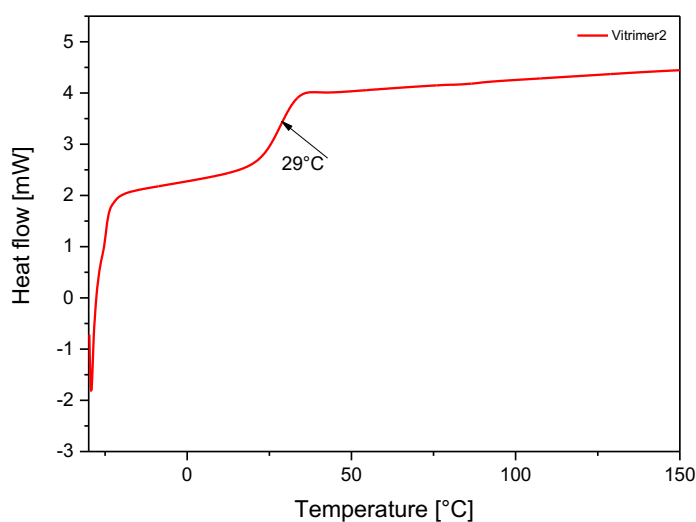


**Figure 51. DSC of Vitrimer 2 (11)**



### *TGA analysis*

The TGA analysis was carried out with a temperature range between 30°C and 600°C in an inert atmosphere. The analysis in Figure 52 shows a residue of 18.2% and good thermal stability since the temperature at which the sample begins to lose weight is around 250°C, and the temperature at which the sample has the maximum weight loss is around 350°C. It is noticeable that the Vitrimer 2 (11) residue in the test (18.2%) is lower than the Vitrimer 1 (9) (28.6%). The lower value is explained by the higher amount of aliphatic chains in the Vitrimer 2 (11) that degrade in nitrogen conditions, resulting in a lower percentage of remaining char after the test.

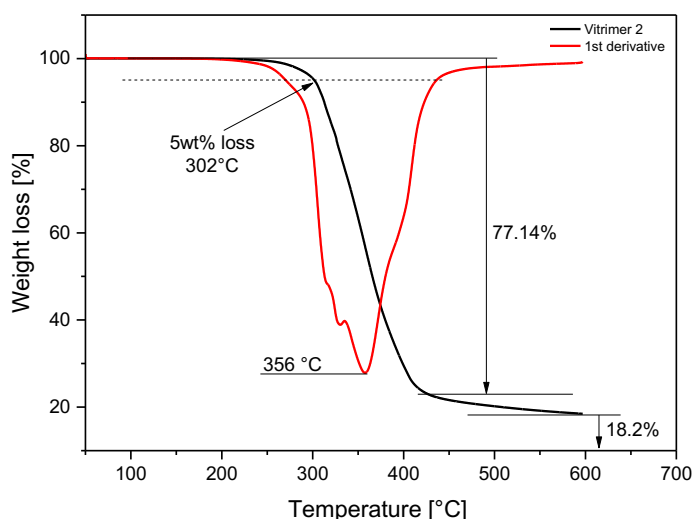


**Figure 52. TGA of Vitrimer 2 (11)**

### *DMA analysis*

The DMA analysis was carried out with a temperature range between -10°C and 100°C. From the analysis, shown in Figure 53, it is possible to notice the temperature of glass transition at 36°C and the storage modulus ( $E'$ ) at 10°C of 2177.70 MPa. Furthermore, the storage modulus ( $E'$ ) at 80°C is 0.98 MPa, lower than the Vitrimer 1 (9) if compared. The explanation of these properties can be found in crosslink density: the structure of the Vitrimer 1 (9) has a higher amount of crosslink density, and this is reflected in the higher storage modulus found after the glass transition temperature. In addition, before the  $T_g$  is expected to have a higher storage modulus because of the higher crosslink density and the higher content of aromatic chain in the Vitrimer 1 (9), but the behaviour is the opposite.

The higher storage modulus in Vitrimer 2 (11) below  $T_g$  can be explained by the higher degree of conversion measured by DSC analysis (see below Figure 55).

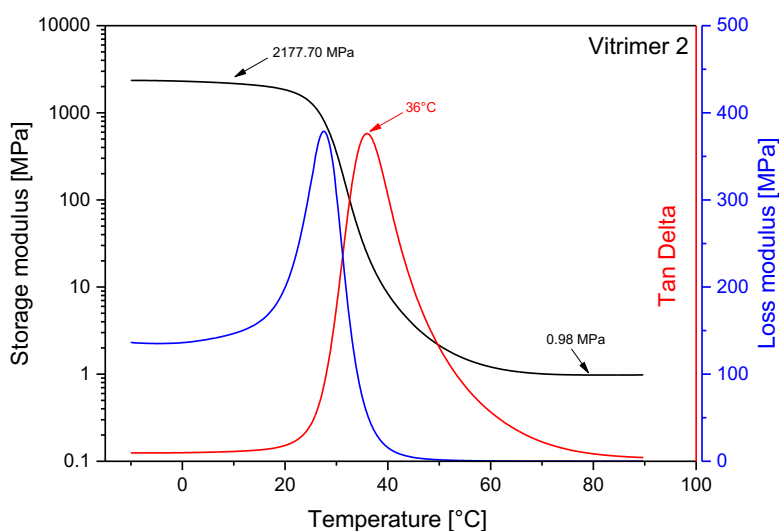


**Figure 53. DMA of Vitrimer 2 (11).**

### *Tensile test*

The Vitrimer 2 (11) tensile tests involved four different samples. In Figure 54 is reported one test as a representative curve. In table 5 are reported the average values of elastic modulus (expressed in MPa), extension at break (expressed as a percentage), and tensile stress break (MPa). It is noticeable in a high dispersion in the data, possibly caused by the fabrication method of the sample. The Vitrimer 2 (11) samples have higher elastic modulus than Vitrimer 1 (9), derived from the higher amount of conversion of the reaction mixture that is visible in Figure 55.

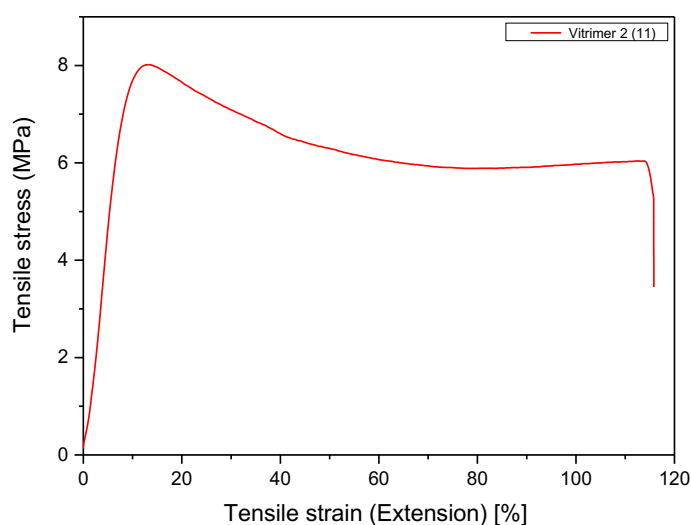


**Figure 54. Tensile test of Vitrimer 2 (11).**

Sample	Elastic modulus (MPa)	Tensile stress at break (MPa)	Extension at break (%)
Vitrimer 2 (11)	115.75±22.10	5.53±0.63 MPa	114.89±15.90

**Table 5. Tensile test of Vitrimer 2 (11)**

#### *Mixture conversion*

Following the same procedure described in the previous paragraph, it has been evaluated the conversion of the reaction mixture of Vitrimer 2 (11) dividing the integral's peak of isothermal DSC (-636 mJ, blue line in image 55) by the integral's peak that corresponds to 100% of conversion (-1264 mJ, red curve in image 55). The operation leads to 50% conversion.

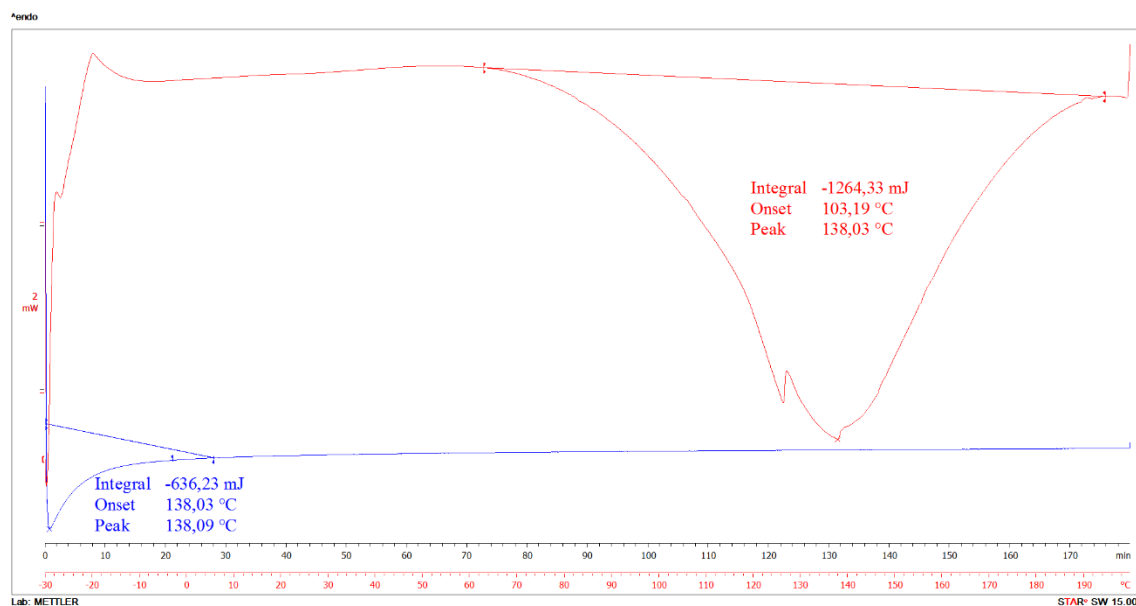


**Figure 55. DSC of reaction mixture (red curve) and isothermal DSC of reaction mixture (blue curve).**

### *Gel content test*

The gel content test was carried out with two different solvents, ethanol (EtOH) and tetrahydrofuran (THF), that solubilise the starting monomer, but does not solubilise the cured polymer. As visible in the table 7, the average gel content of Vitrimer 2 (11) in both cases is around 77%, and from the Figures 56 and 57 is visible that the polymer dissolved partially in the solvent.

The gel content value, lower than Vitrimer 1 (9), may be attributed to the higher steric hindrance of the monomer 2 (7), which can prevent the reaction of all the functional groups in the molecule, leading to the formation of oligomers, that are dissolved in the solvent. Furthermore, monomer 2 (7) has three functional groups (-OH) that react with TMP-TGE, while monomer 1 (5) has two. The TMP-TGE contains three functional groups, and in the case of the Vitrimer 1 (9) there is an excess of epoxide groups. In this case, the functional groups of monomer 2 (7) are equal to those of TMP-TGE, leading to a minor percentage of -OH groups reacted and a minor gel content test. The theory would require more in-depth studies.

Sample	Average gel content (%) in EtOH	Average gel content (%) in THF
Vitrimer 2 (11)	77.0±0.3	77.6±1.3

**Table 7. Gel content test of Vitrimer 2 (11).**

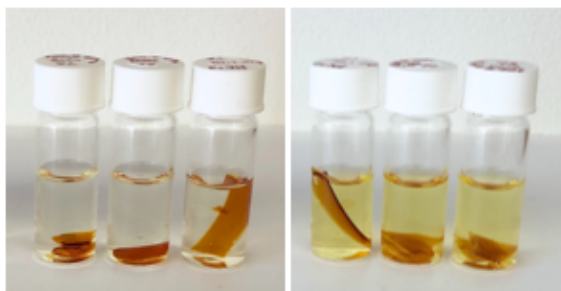


**Figure 56. Gel content test of Vitrimer 2 (11) in EtOH, start and after 3 days.**

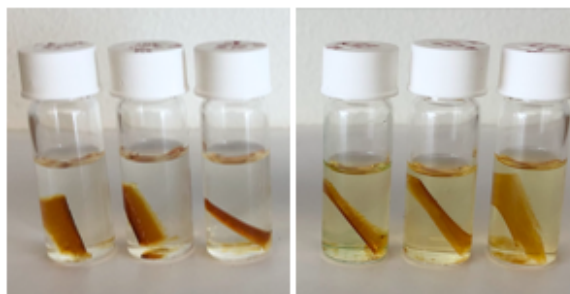


**Figure 57. Gel content test of Vitrimer 2 (11) in THF, start and after 3 days.**

### *Chemical resistance*

Seven sample of Vitrimer 1 (9) were placed in seven different vials containing solvents and the chemical resistance was tested. The samples weighted 50 mg, and the solvents were acetone, tetrahydrofuran (THF), dimethylformamide (DMF), dicloromethane (DCM), sodium hydroxide (NaOH) 1M, ethanol (EtOH) and dimethyl sulfoxide (DMSO). After two days the Vitrimer dissolved partially only in DMSO and DMF, showing an excellent chemical resistance in the most common solvents (Figure 58).

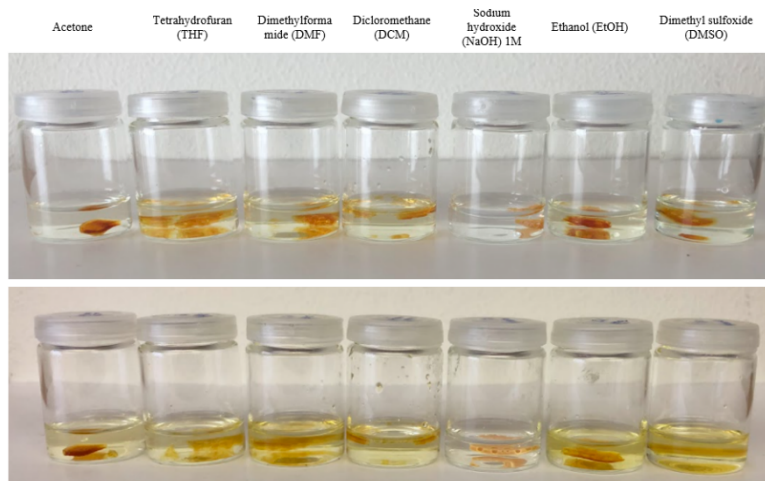


**Figure 58. Chemical resistance test, start and after 2 days.**

### Chemical recycling

With the same procedure described in for Vitrimer 1 and the same purpose, it has been conducted a chemical recycling of Vitrimer 2 (11). Like the previous Vitrimer, it has been proved through  $^1\text{H}$  NMR analysis conducted during the degradation, that the main peaks of the starting materials appear (Figures 59 and 60).

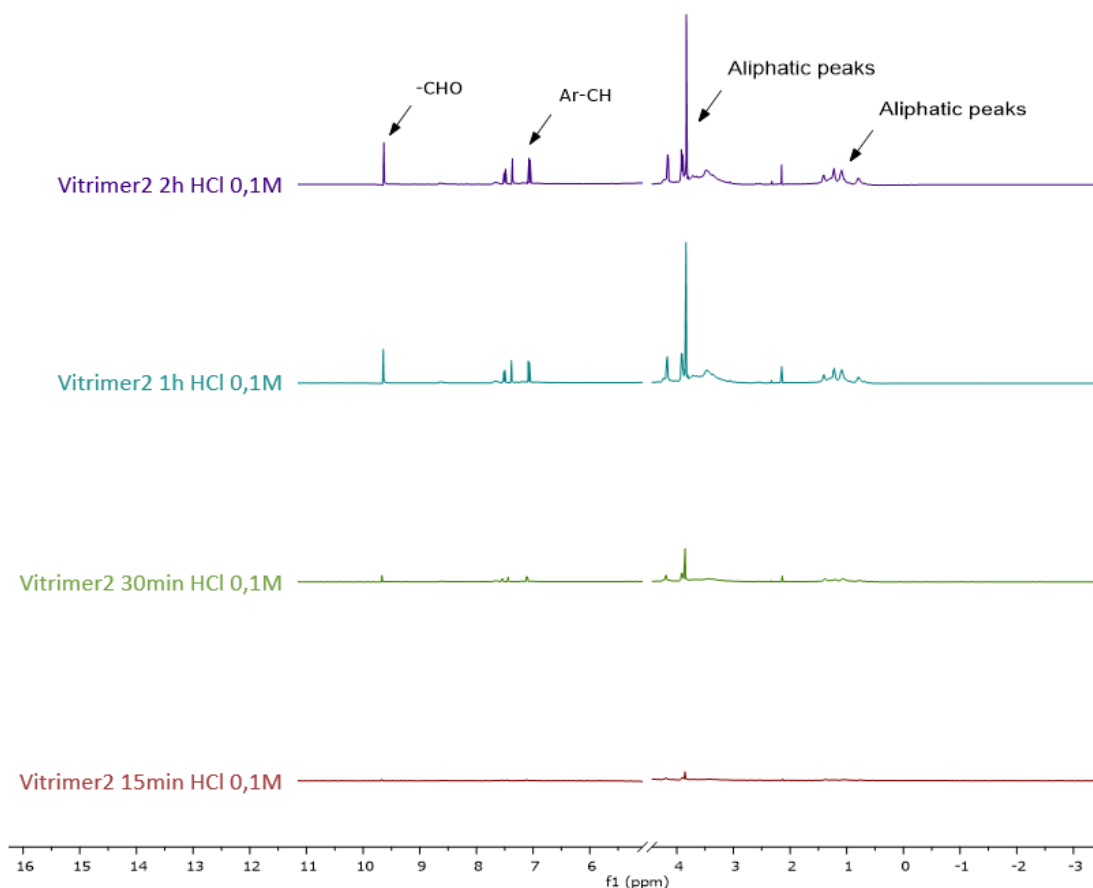


**Figure 59.** Comparison of NMR spectra of Vitrimer 2 (12an) in HCl 0.1 M during time.

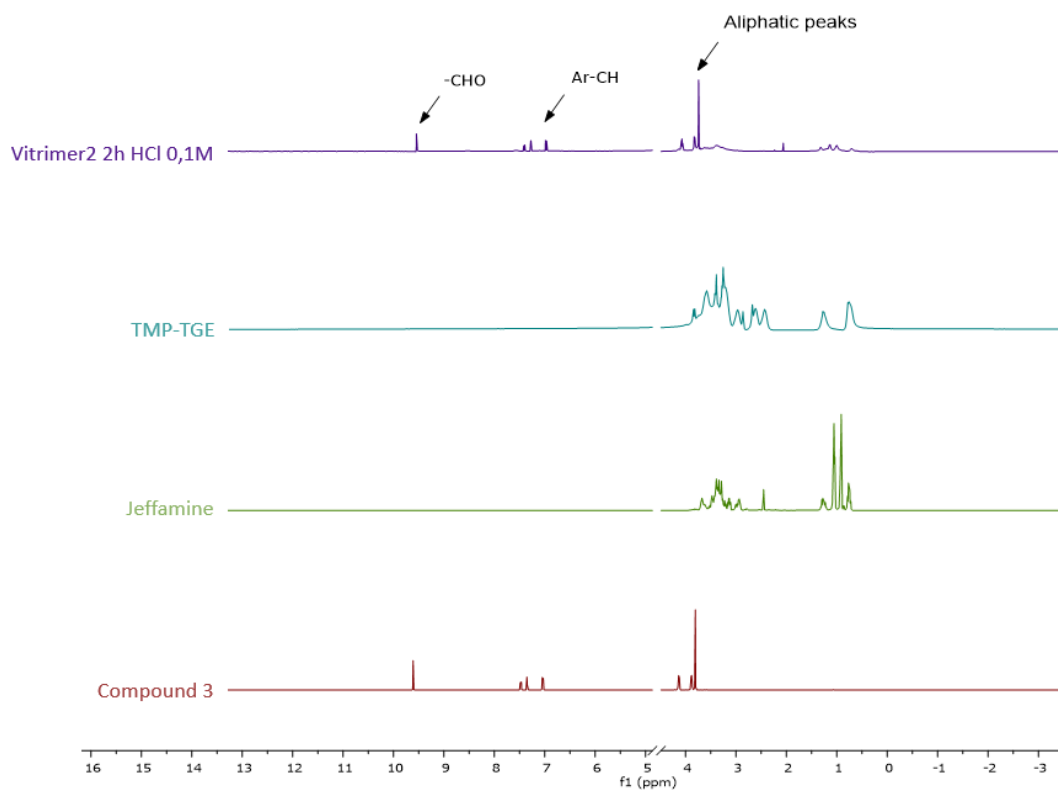


**Figure 60.** Comparison of  $^1\text{H}$  NMR spectra of Vitrimer 2 (11) after 2h in HCl 0.1 with precursors.

### 3.3.3 Synthesis of Vitrimer 1 (9) and Vitrimer 2 (11) with different ratio

#### Vitrimer 1 (9)

The effect of diol-epoxy molar ratio was investigated for Vitrimer 1 (9) changing the ratio of starting materials. The different ratios are shown in Table 8, and the result is shown in figure 61.

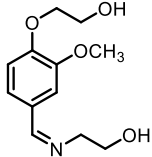
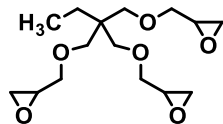
		
a	1 monomer	1.3 TMP-TGE
b	1 monomer	1.2 TMP-TGE
c	1 monomer	1.1 TMP-TGE
d	1 monomer	1 TMP-TGE
e	1.1 monomer	1 TMP-TGE
f	1.2 monomer	1 TMP-TGE
g	1.3 monomer	1 TMP-TGE

Table 8. Different ratios of starting materials.

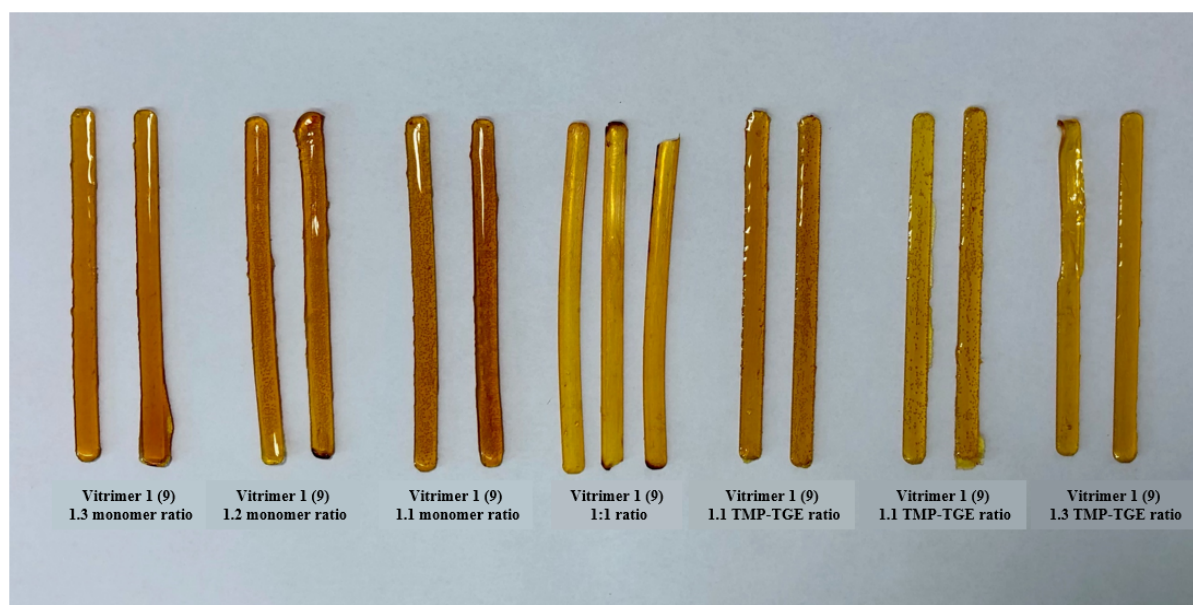
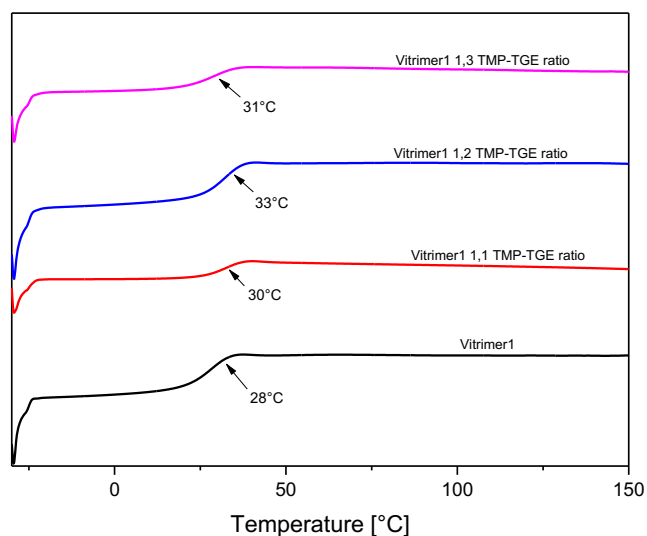


Figure 61. Different ratios of Vitrimer 1 (9).

All the formulations were analysed through the DSC analysis, in order to find a correlation in the glass transition temperature based on the ratio, but, as visible in the Figures 62 and 63, the  $T_g$  does not change remarkably with the variation of the ratio, but is shown a slight decrease of  $T_g$  in the formulations that contains more monomer. This behaviour can be attributed to the decrease of crosslinking reaction that the higher amount



of monomer gives to the final structure. To confirm this theory, more studies would be required.



**Figure 62. DSC analysis of Vitrimer 1 (9) changing the ratio of TMP-TGE.**

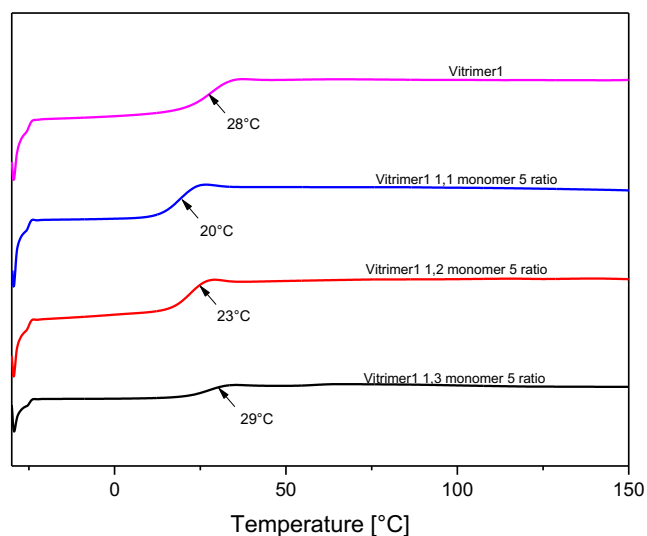


**Figure 63. DSC analysis of Vitrimer 1 (9) changing the ratio of monomer.**

Samples with a different ratio showed lower mechanical characteristics than the starting Vitrimer, breaking easily. The only sample with characteristics comparable to the original Vitrimer is the formulation with 1.1 TMP-TGE ratio.

In order to characterize them, they have been made tensile tests and DMA.

From the tensile test in Figure 64 and the relative Table 9, it can be observed a modulus decrease with respect to the original polymer of an order of magnitude. In contrast, the tensile stress at break and the extension at break remained almost unchanged.

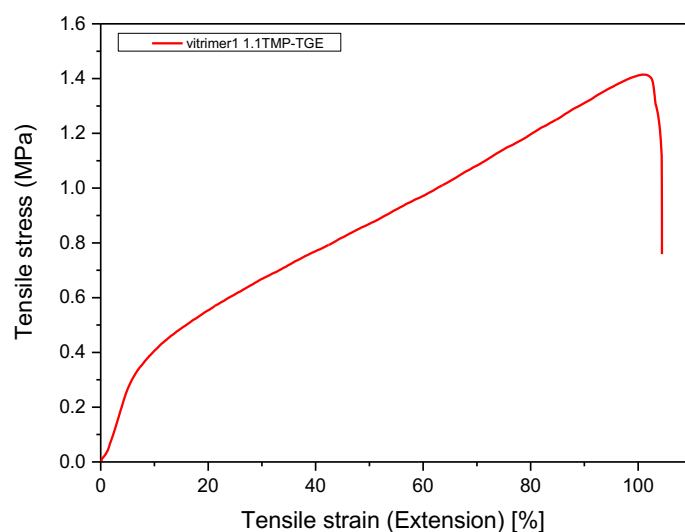


**Figure 64. Tensile test of Vitrimer 1 (9) 1.1 TMP-TGE ratio.**

Sample	Elastic modulus (MPa)	Tensile stress at break (MPa)	Extension at break (%)
Vitrimer 1 (9) 1.1 TMP-TGE ratio	1.36±0.15	1.18±0.16 MPa	101.76±5.11

**Table 9. Tensile test of Vitrimer 1 (9) 1.1 TMP-TGE ratio.**

As expected, also DMA analysis (Figure 65), shows lower properties than Vitrimer 1 (9) with 1:1 ratio, in fact, E' modulus of Vitrimer 1 (9) 1.1 TMP-TGE ratio measured at 10°C of about 50%.

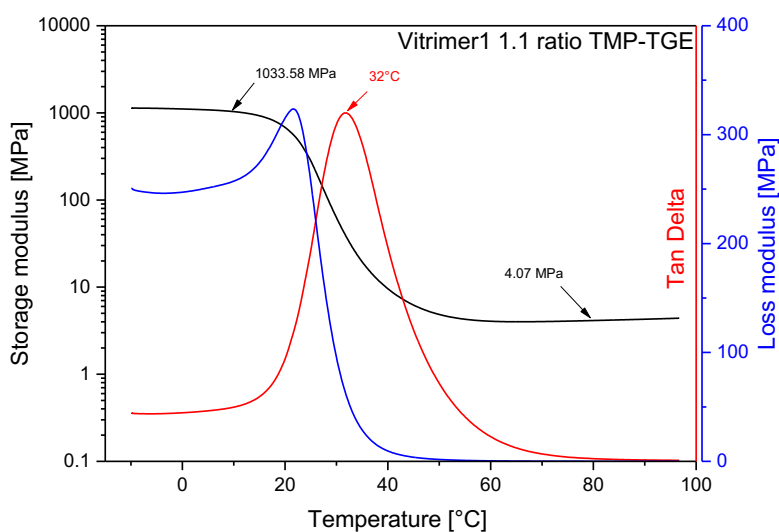


**Figure 65. DMA of Vitrimer 1 1.1 TMP-TGE ratio.**

## Vitrimer 2 (11)

Following the same procedure exposed in the previous paragraph, other sample of Vitrimer 2 (11) were synthesized changing the ratio of starting materials. The different ratios are shown in Table 10, and the result is shown in Figure 66. In this case none of the samples was appropriate to be studied, both the samples had lower mechanical characteristics than the starting Vitrimer.

a	1.1 monomer	1 TMP-TGE
b	1 monomer	1 TMP-TGE
c	1 monomer	1.1 TMP-TGE

**Table 10. Different ratios of Vitrimer 2 (11).**



**Figure 66. Different ratios of Vitrimer 2 (11).**

All the formulations were analysed through DSC (Figure 67). It is noticeable a decrease in glass transition temperature in Vitrimer 2 (11) with 1.1 TMP-TGE ratio, probably due to the increasing of aliphatic chains that are obtained with this specific ratio, which brings to a lower  $T_g$ . Additional studies are needed to confirm this hypothesis.

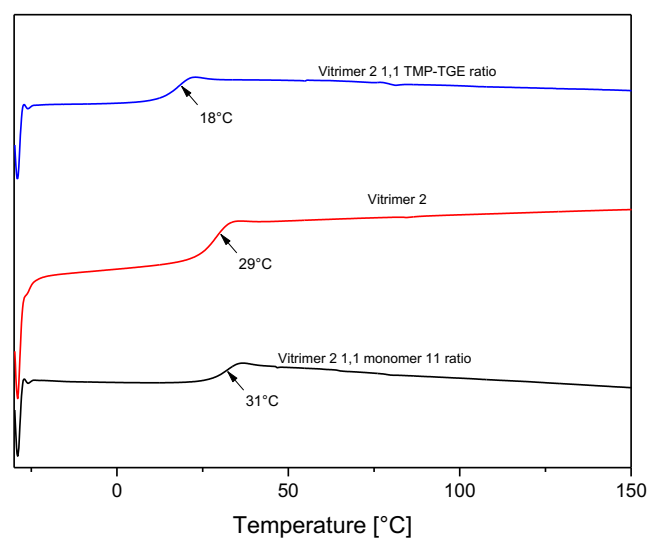


**Figure 67. DSC analysis of Vitrimers 2 (11) changing ratio of reactants.**

### ***3.4 Thermoset polymers – reprocessing***

All the studied formulation, Vitrimer 1 (9) and Vitrimer 2 (11) and Vitrimer 1 (9) 1.1 TMP-TGE, were reprocessed. The method used consists in cutting the samples in small pieces of about 5 mm each and place them in a mold. The mold was then placed inside a hot press (Figure 68) and maintained for one hour at 130°C with a pressure of 75kN. The result of the process is a less flexible material than the non-reprocessed one with a good transparency, as visible in Figures 69 and 70.



**Figure 68. Hot-press machine.**



**Figure 69. Vitrimer 1 (9) before and after hot press.**



**Figure 70. Vitrimer 2 (11) after hot press.**

Both formulation of Vitrimer 1 (9) were characterized again, while the reprocessed-Vitrimer 2 (11) was too brittle to be characterized. The result, in the reprocessed samples, was a higher tensile modulus, higher tensile stress at break and lower extension at break (Figures 71 and 72 and Tables 11 and 12). The properties can be explained by the increasing of degree of crosslinking during the hot processing, resulting in higher stiffness and lower ductility of the material.

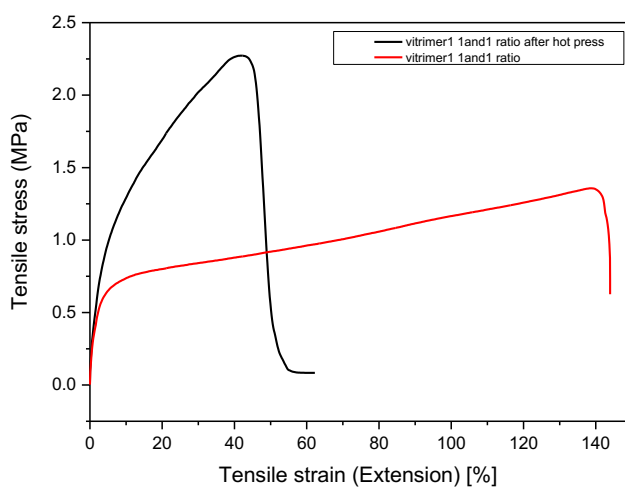


**Figure 71. Tensile tests of Vitrimer 1 (9) and reprocessed-Vitrimer 1 (9).**

Sample	Elastic modulus (MPa)	Tensile stress at break (MPa)	Extension at break (%)
Vitrimer 1 (9)	11.97±1.65	1.20±0.12 MPa	139.31±6.94
Reprocessed Vitrimer 1 (9)	25.44±5.68	2.55±0.74 MPa	47.60±10.10

**Table 11. Tensile test of reprocessed Vitrimer 1 (9).**

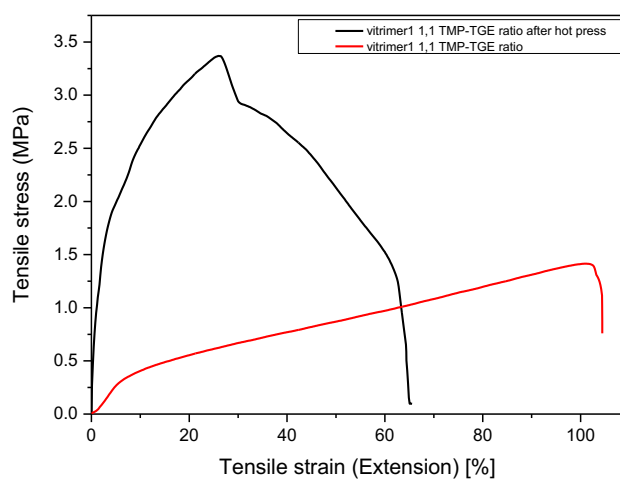


**Figure 72. Tensile tests of Vitrimer 1 (9) 1.1 TMP-TGE and reprocessed-Vitrimer 1 (9) 1.1 TMP-TGE.**

Sample	Elastic modulus (MPa)	Tensile stress at break (MPa)	Extension at break (%)
Vitrimer 1 (9) 1.1 TMP-TGE	1.36±0.15	1.18±0.16 MPa	101.76±5.11
Reprocessed Vitrimer 1 (9) 1.1 TMP-TGE	55.40±10.96	4.29±0.73 MPa	54.17±4.29

**Table 12. Tensile test of reprocessed Vitrimer 1 (9) 1.1 TMP-TGE.**





## Chapter 4: Conclusions

The thesis is focalized on the synthesis of alternatives to the conventional fossil-based polymers, producing new bio-based polymers with comparable characteristics that can be easily recycled and reprocessed.

Two biobased, chemically recyclable imine linear polymers and two biobased thermally curable, chemically recyclable, and thermal reprocessable imine Vitrimers were successfully synthesized through chemical modification of vanillin.

The vanillin was made to react with ethylene carbonate to obtain extended vanillin, which has higher reactivity than the vanillin itself. The extended vanillin was the starting material for both the monomer synthesized that both contained amine groups, inserted in the structure by reactions with aminoethanol and Jeffamine 440 (a triamine compound). The monomers were, in turn, the starting materials for the polymers. The two hydroxyl groups of the monomer 1 (5) were reacted to make all the three polymers derived from it. The polyurethane was made by reaction with a diisocyanate, and the polyester was made by reaction with dimethyl succinate.

The Vitrimer's crosslinking reactions were made using trimethylolpropane triglycidyl ether (TMP-TGE). The amine bond imparted thermal curability, confirmed by the decrease in FTIR analysis of the amine bond after exposure to heat.

All the steps of the reactions were confirmed by spectroscopy analysis such as  $^1\text{H}$  NMR,  $^{13}\text{C}$  NMR, and FTIR.

The linear polymers showed high thermal stability from the TGA analysis, showing a  $T_5$  at around  $250^\circ\text{C}$ , a value comparable to the conventional polyurethanes and polyesters [24-27].

The cured thermosets showed optimal stability in common solvents, good thermal stability ( $T_5$  is approximately  $300^\circ\text{C}$ ), and high storage modulus at  $10^\circ\text{C}$  (1500 MPa for the Vitrimer 1 and 2000 MPa for the Vitrimer 2).

For all the materials, the presence of the imine bond allows easy recycling in acidic conditions at room temperature through the breaking of the imine bond.

Exploiting the amide bond, all the synthesized materials can be easily recycled in weak acidic conditions in a short time at room temperature, leading to the obtaining of the

starting compounds, as visible in the  $^1\text{H}$  NMR spectra of the chemically recycled polymers.

The properties that have been studied in this work show promising characteristics of Schiff-base polymers.

Moreover, both the thermosets can be thermally reprocessed by cutting them into small pieces and subsequent hot pressing, and after reprocessing, the Young's modulus increases. The increase is due to the additional crosslinking reactions in the hot press since the unreacted monomer creates additional crosslink bonds.

Remarkably, Vitrimers materials have a promising potential for replacing petroleum-based thermosets [28]. Furthermore, they have a significant advantage in terms of reprocessability, combining the possibility of dissolving them in the starting materials using appropriate solvents with the possibility of thermal reprocessing using hot press. The possibility of recycling potentially leads to complete recovery at the end of life of these materials, which is impossible for conventional thermosets.





## Bibliography

1. *The New Plastics Economy: Rethinking the Future of Plastics & Catalysing Action*  
Available online: <https://www.ellenmacarthurfoundation.org/publications/the-new-plastics-economy-rethinking-the-future-of-plastics-catalysing-action> (accessed on April 2022).
2. Sardon, H.; Dove, A.P. *Plastics Recycling with a Difference*. Science 2018, 360, 380–381, doi:10.1126/science. aat4997.
3. PlasticsEurope. *Annual Production of Plastics in Europe from 1950 to 2020 (in Million Metric Tons)*. Statista, Statista Inc., 20 Dec 2021, <https://www-statista-com.ezproxy.biblio.polito.it/statistics/987838/plastics-production-volume-in-the-eu-28/>.
4. AlMaadeed A.A.A, *et al*, Chapter 1, Polymers to improve the world and lifestyle: physical, mechanical, and chemical needs, *Polymer Science and Innovative Applications*, Elsevier, 2020.
5. Shrivastava A. *Introduction to plastics engineering*. William Andrew, 2018.
6. Biron M. *et al*, *Material Selection for Thermoplastic Parts: Practical and Advanced Information*, William Andrew, Oxford, 2020.
7. Ebewele R.O. *Polymer science and technology*, CRC press, 2000.
8. Thomas E.L., *Structure and properties of Polymers*, Wiley, 1993.
9. Kloxin C.J. *et al*, *Covalent Adaptable Networks (CANs): A Unique Paradigm in Crosslinked Polymers*. Macromolecules, 2010.
10. Gamardella F., *et al*, *Towards the Recyclability of Thermosetting Polymers*, Tarragona, 2020.
11. Denissen W., *et al*, *Vitrimers: permanent organic networks with glasslike fluidity*, Chem. Sci, 2016.
12. Montarnal D., *et al*. *Silica-like malleable materials from permanent organic networks*. Science, New York, 2011.
13. Elling B.R, *et al*, *Reprocessable Cross-Linked Polymer Networks: Are Associative Exchange Mechanisms Desirable?* ACS, Cent. Sci. 2020.
14. Hayashi M. *Implantation of Recyclability and Healability into Cross-Linked Commercial Polymers by Applying the Vitrimer Concept*, Polymers vol. 12,6 2020
15. Winne J.M., *et al*, *Dynamic covalent chemistry in polymer networks: a mechanistic perspective*, Polymer Chemistry, 2019.

16. Milosevic M., *Internal Reflection and ATR Spectroscopy*, chapter 1, Introduction to spectroscopy, Wiley, 2012.
17. Hinton-Sheley, Phoebe. *ATR-FTIR: An Overview*. AZoLifeSciences. 30 March 2022. <<https://www.azolifesciences.com/article/What-is-ATR-FTIR.aspx>>.
18. Günther H., *NMR Spectroscopy: Basic Principles, Concepts, and Applications in Chemistry*, (3rd ed.). John Wiley & Sons, 2013.
19. Deb P.K., *et al*, *Pharmaceutical and Biomedical Applications of Polymers*, chapter 6.5.4, Size Exclusion Chromatography, Academic Press, 2019.
20. T. Hatakeyama T., *et al*, *Thermal Analysis Fundamentals and Applications to Polymer Science*, 2nd ed., John Wiley & Sons, New York, 1999.
21. Web site - <http://www.ipfdd.de/en/research/institute-of-macromolecular-chemistry/center-macromolecular-structure-analysis/analytical-methods/thermal-analysis/thermogravimetric-analysis-tga/>, [online], April 2022.
22. Web site, <https://pslc.ws/italian/dsc.htm>, [online], September 2021.
23. Menard, K.P. (2020). *Dynamic Mechanical Analysis* (3rd ed.). CRC Press, 2020.
24. Trovati G., *et al*, *Characterization of polyurethane resins by FTIR, TGA, and XRD*. *J. Appl. Polym. Sci.*, 2010.
25. Valdés B., *et al*, *Synthesis and Characterization of Isosorbide-Based Polyurethanes Exhibiting Low Cytotoxicity Towards HaCaT Human Skin Cells*, *Polymers*, 2018.
26. Stumbé J., *et al*, *Hyperbranched polyesters based on adipic acid and glycerol*. *Macromol Rapid Commun.*, 2004.
27. Arza C., *et al*, *Synthesis, Thermal Properties, and Rheological Characteristics of Indole-Based Aromatic Polyesters*, *ACS Omega*, 2019.
28. Xu Y., *et al*, *Photocurable, Thermally Reprocessable, and Chemically Recyclable Vanillin-Based Imine Thermosets*, *ACS Sustainable Chemistry & Engineering*, 2020.